Physics – Uspekhi **65** (2) 163 – 188 (2022)

INSTRUMENTS AND METHODS OF INVESTIGATION PACS numbers: **34.80.–i**, 34.80.Ht, **34.90.+q**

State of the art in dissociative electron attachment spectroscopy and its prospects

S A Pshenichnyuk, N L Asfandiarov, A S Vorob'ev, Š Matejčík

DOI: https://doi.org/10.3367/UFNe.2021.09.039054

Contents

Abstract. The latest achievements are presented in experimental and theoretical studies of resonance scattering of low-energy (0–15-eV) electrons from molecular targets in a gas phase resulting in the formation and decay of negative ions. The focus is on dissociative electron attachment spectroscopy for studying the microsecond dynamics of molecules containing an excess electron. Some studies of fundamental processes in isolated negative ions containing up to several electronvolts of excess energy are briefly described, and the possibility of using the results in interdisciplinary fields is discussed. A goal of the paper is to attract attention to the above-mentioned studies, which are rapidly developing abroad but only scarcely presented in the domestic literature.

Keywords: resonance electron scattering, shape resonance, vibrational Feshbach resonance, long-lived molecular negative ions, dissociative attachment, electron autodetachment, electron-induced processes, spectroscopy, mass-spectrometry

S A Pshenichnyuk [(1, a)], **N L Asfandiarov** [(1, b)], **A S Vorob'ev** [(2, c)], **Š Matejčík** [(3, d)]
[(1)] Institute of Molecule and Crystal Physics, Ufa Federal Research Center, Russian Academy of Sciences, prosp. Oktyabrya 151, 450075 Ufa, Russian Federation
[(2)] Moscow Institute of Physics and Technology (National Research University), Institutskii per. 9, 141701 Dolgoprudnyi, Moscow region, Russian Federation
[(3)] Department of Experimental Physics, Comenius University, Mlynská dolina F2, 84248 Bratislava, Slovakia
E-mail: [(a)] sapsh@anrb.ru, [(b)] nail_asf@mail.ru, [(c)] vendas@list.ru, [(d)] matejcik@fmph.uniba.sk

Received 21 August 2020, revised 30 September 2021
Uspekhi Fizicheskikh Nauk **192** (2) 177 – 204 (2022)
Translated by M Sapozhnikov

1. Introduction

1.1 Brief information on dissociative electron attachment

The ability of many atoms and molecules to attach an additional electron, known since the early 20th century [1, 2], can lead under certain conditions to the formation of bound states — negative ions (NIs) with lifetimes from femtoseconds to milliseconds. This process occurs during the transfer of an electron from a neutral particle or other NI [3, 4] or due to the attachment (the term 'adhesion' [5] is also used in the Russian literature) of free electrons. The latter process can be considered to be low-energy electron scattering from molecules [6] at energies significantly lower than the ionization potential of target molecules and the direct formation energy of ion pairs. If the incident electron energy is sufficient for

occupying one of the vacant orbitals of a target molecule, we are dealing with resonance scattering and the formation of short-lived NI states which can decay by dissociating into fragments (dissociative electron attachment (DEA)) or by spontaneous ejection (autodetachment) of the attached electron [7, 8]. In this case, the scattering cross section drastically increases, and narrow maxima corresponding to the formation of bound states are observed on a gradually decreasing background of the potential scattering cross section depending on the electron energy. The development of experimental methods and the history of resonance attachment studies began from the second half of the 20th century [9–11] simultaneously with the development of basic theoretical concepts in this field [6, 12, 13].

1.2 Essential literature

Our review does not claim to be a full consideration of the problem under study, and therefore we only briefly mention in this section fundamental work which can be useful for our readers. After the publication of fundamental studies by Schulz [10, 11] containing basic information on resonance electron capture by atoms and diatomic molecules, numerous monographs and reviews have been published in this field. Note among them the books by Christophorou [14] and Illenberger [15] describing all the numerous experimental and theoretical methods used in these studies. The authors of book [16] explain how the methods developed in this field can be used to solve problems appearing in various, sometimes unexpected, fields, such as plasma physics, micro- and nanoelectronics, nanolithography, DNA investigations, and atmospheric and interstellar medium physics. Theoretical investigations are considered in work on the fundamentals of physics of electron-molecule collisions [17] and applications of *ab initio* methods [18]. The main results and stages of the development of negative ion mass spectrometry of resonance electron attachment (NIMS REA) in Ufa are described in Khvostenko's work [19, 20].

The unique experimental equipment in electron impact spectroscopy is described in Allan's review [21]. Note that a trochoidal monochromator [22, 23] is the most convenient instrument for reducing the energy spread of initial electrons. Review [24] describes theoretical approaches to studying electron attachment (the projection operator method, Faddeev equations, the R-matrix theory) and some experimental methods under conditions of pair collisions (collisional ionization of Rydberg atoms, photoionization of inert gases, the crossed beam method) and multiple collisions (the swarm method, the Langmuir probe, pulsed radiolysis). Threshold phenomena in the electron scattering cross section studied with ultrahigh resolution (microelectronvolts) are described in [25, 26]. Fabrikant [27] considered methods of the R-matrix theory explaining many experimental observations: from the behavior of cross sections at low temperatures and threshold effects to the temperature dependence of the electron attachment rate. The structure and dynamics of atomic NIs are presented in review [28]. Note also recent studies [29–31].

1.3 Topical applications of results

The elementary process of electron capturing by an isolated molecule is of interest from both the fundamental and applied points of view [14–16]. The formation of molecular negative ions (MNIs) is governed by resonance mechanisms [10, 11] and described in terms of the energy and symmetry of vacant molecular orbitals (MOs), which facilitates the development of quantum-chemical methods [32, 33]. MNI decomposition due to electron autodetachment or dissociation into fragments is determined by the fundamental characteristics of a target molecule: the number of vibrational degrees of freedom, the spatial structure, the vibrational state [34], and the electron affinity. The is a manifestation of a sequence of quantum processes, including electron capture by one of the vacant MOs, electronic excitation energy transfer to vibrational modes [35], the redistribution of excess energy among MNI vibrations, its concentration on a certain coordinate of the reaction, and MNI dissociation [36]. Thus, DEA studies provide new information on the structure and dynamics of microscopic systems.

The electron attachment determines a broad scope of phenomena from chemical reactions, properties of gas dielectrics [37], reactions in the atmosphere [38] and the interstellar medium [39, 40] to electronic processes in thin films and redox reactions. The results are important in many fields, such as low-temperature plasma physics [41], biophysics, atmosphere physics, molecular electronics, medicine, toxicology and pharmacology, and materials [42] and environmental [43] science and are used in scientific and applied problems in radiation biology [44], to control chemical reactions on surfaces [45], and in studies of the origin of life [46]. Thus, DEA studies should be performed in order to understand fundamental natural phenomena at the molecular level and applications in various interdisciplinary problems.

1.4 Current state of domestic studies

The DEA studies being performed at present in Ufa are unique for our country, which is not, however, related to the loss of their applicability, as is illustrated in Fig. 1, where the main foreign scientific centers working in this field are shown. This direction in Russian science is poorly known, which probably explains the fact that reviews [47, 48], devoted to mechanisms of the biological action of radiation and, in particular, pointing out the necessity of a search for new radiation-induced factors, do not mention the DEA mechanism, whose contribution to chromosome aberrations was established [49] (see Section 4.1 below).

It seems that a poor state of DEA studies in our country is mainly explained by recent political events in the history of Russia. The NIMS REA method was developed in Ufa in the 1960s [19, 20] simultaneously with the efforts of foreign researchers [10, 11]. More detailed historical information can be found in [50]. A decade later, reviews were published in *Sov. Phys. Usp.* [51, 52] and in foreign journals [7, 21]. Aside from the Ufa school, researchers from Novosibirsk [53], Vladivostok [54], Uzhgorod [55, 56], Moscow [57], Leningrad [58], Riga [59], Cheboksary, and Minsk [60, 61] were involved in this field. The collapse of the USSR catastrophically prevented the development of a new field of science at that time.

In our country, the latest review on DEA was published more than 20 years ago [5]. New results in this field were published abroad in monograph [31] and reviews [29, 62]. Note also the declared renaissance in investigations of resonance scattering [63] and numerous publications presented below. The above consideration suggests that the discussion of some achievements in the field of resonance scattering in domestic scientific literature is absolutely necessary.

Figure 1. (Color online.) Some research groups involved in studies of resonance electron scattering and processes of production and decay of negative ions. The only group actually involved in such studies in our country is indicted in red.

1.5 Structure of the review

This review is not supposed to be a comprehensive discussion of the material but instead presents the authors' view of the subject under study. We considered studies published mainly over the last two decades, i.e., after paper [5], and presenting, in our opinion, interesting and new areas of investigations. In Section 2, experimental studies of electron-molecule collisions in the resonance capture regime are described, the technique of Ufa experiments is presented as an example of using a sector magnetic field as a mass analyzer, the recent method of velocity slice imaging is mentioned, and the use of polarized electrons and the possibility of detecting neutral fragments is discussed. In Section 3, we considered briefly theoretical approaches, attempts at DEA simulations, and calculations of molecular characteristics by the methods of the density functional theory (DFT). The main focus is devoted to the use of simple methods describing experimental results for quite large molecules, which is impossible within the framework of more rigorous theoretical approaches. In Section 4, new results are considered, including the fundamental possibility of estimating electron affinity from MNI lifetimes, which can be considered a promising development in DEA spectroscopy, which involves, however, the upgrading of experimental equipment. In Section 4, also described are studies having applications in radiobiology. The results of DEA studies for biologically active molecules and structural elements of organic electronics are presented.

Thus, aside from some solved problems related to new directions in the experimental technique (Sections 2.2 and 2.3) and the development of calculation methods for interpreting experimental results (Sections 3.2–3.4), our review concerns a number of fundamental questions related to the formation and decomposition of NIs in pair collisions of electrons with isolated polyatomic molecules. In our opinion, the most important of the problems unsolved so far is the measurement of the nonradiative relaxation rate (internal conversion) of shape resonances resulting in the rapid stabilization of short-lived femtosecond NI states. In addition, the rates and paths of the redistribution of internal energy and vibrational relaxation in long-lived (microseconds) molecular anions should be found. These processes determine the dynamic behavior and decomposition of NIs caused by electron autodetachment and dissociation into fragments (Sections 3.5, 3.6, 4.5). However, their description is complicated due to the obvious manifestation of anharmonicity and due to the difference between vibrational spectra of NI and neutral molecules. The solution to these problems is complicated not only by the presence of an additional electron in the molecular system and a large excess of internal energy (up to a several eV), but also by the fact that, at present, of interest are mainly polyatomic structures whose calculations require considerable computer time. Note that great progress was achieved in the understanding of long-range effects and the formation of nonvalent NI states, which are in many cases the transient states providing the initial delay of an electron near a target molecule and giving rise to vibrational Feshbach resonances observed in the spectra of transmitted electrons as narrow peaks (tenths of eV) with energies below the first shape resonance (Section 3.1).

The use of the results of DEA spectroscopy in simulations of biological processes at the molecular level (Sections 4.1 and 4.2) and for understanding electronic processes in elements of organic electronics (Section 4.3) requires solving the problem of extrapolating the results of gas-phase experiments to a condensed environment consisting of many phases and components. At present, this problem is far from a solution, which requires the use of several experimental methods, including studies of electrochemical processes in solutions

and electron capture by molecules introduced into clusters in combination with simulations of electron scattering in the presence of an environment. A separate problem is the development of a new method for estimating the electron affinity by measuring the mean electron-autodetachment time (Section 4.4), which simultaneously solves the problem of interpreting the results of DEA spectroscopy under real experimental conditions, i.e., in the presence of the distribution of target molecules over vibrational states and of electrons over energies. In the conclusion, the outlook for the development of this field is considered and new problems, including interdisciplinary ones appearing in these studies, are discussed.

2. Experimental methods for studying resonance electron attachment

2.1 Electron swarm method and the crossed beam technique

Electron attachment by molecules can be studied by two methods: the electron swarm method (or the electron cloud method in the domestic literature) and the crossed beam technique described in Section 2.4. Work based on the first method played a considerable role in the past in electron attachment studies [64, 65]. The number of such studies in the last two-three decades has noticeably been decreasing. The electron adhesion to molecules in swarm experiments is studied at pressures of about 1 Torr, where the flowing afterglow [66] or electron mobility in homogeneous electric fields is observed by the pulsed Townsend method. The Townsend method was developed in the last decade by groups in Mexico [67–71], Poland [72], and Serbia [73, 74]. Researchers in Switzerland recently used the Townsend method to study the transport and kinetics of electron interactions in gases [75, 76] to determine transport parameters of electrons and ions, including the drift velocity, the total electron-molecule collision cross section, and the capture cross section. Electrons move in a homogeneous electric field in a buffer gas with negative electron affinity (inert gases, N_2, CO_2) at a low concentration of molecules under study. Electron sources work based on the photoelectric effect using a nanosecond UV laser.

Polish researchers used the Townsend method to measure the electron attachment rate for halogen-containing compounds by studying the dependence of an NI signal on the molecular concentration [77–79]. The method of ion mobility spectrometry uses drift tubes [80–83] at high pressures close to atmospheric pressure. The electron source is a radioactive element, for example, beta radiation from ^{63}Ni or a photocathode irradiated in the UV range. Electron capture is also studied in a negative corona discharge in inert gases. The electron-molecule adhesion rate can be determined from the dependence of the electron current on molecular concentration and also by the detection moment of NIs moving more slowly than electrons, which allows their nature and the capture rate to be established.

The development of beam experiments is mainly determined by the use of time-of-flight mass spectrometers and the velocity slice imaging technique, which can be applied for studying not only the electron capture kinetics but also the dynamics of this process by determining the symmetry of the states of transient negative ions. A great contribution to the application of the time-of-flight technique was made by Indian researchers [30, 84–86], who used a crossed beam device and a linear mass spectrometer to measure the absolute partial DEA cross sections. Molecules in excited vibrational states were studied using a laser [84–86]. A time-of-flight mass spectrometer containing several segments to compensate the magnetic field of an electron source manufactured in Freiburg, Switzerland used for measuring effective DEA cross sections is presently operating in Prague [87–89].

2.2 Velocity slice imaging

This method is based on velocity map imaging developed for studying photoionization [91–93]. However, in the case of photonic processes, the experiment is much simpler than for electron-induced reactions. Indian researchers [86, 94, 95] have used a position-sensitive detector to measure kinetic energies and the angular distribution of NIs. Anions moving with the same momentum form a so-called Newton sphere, resulting in a spherical distribution in the velocity space, as shown in Fig. 2. The kinetic energy of NIs and their formation process can be determined from the size of the image of this sphere in the position-sensitive detector.

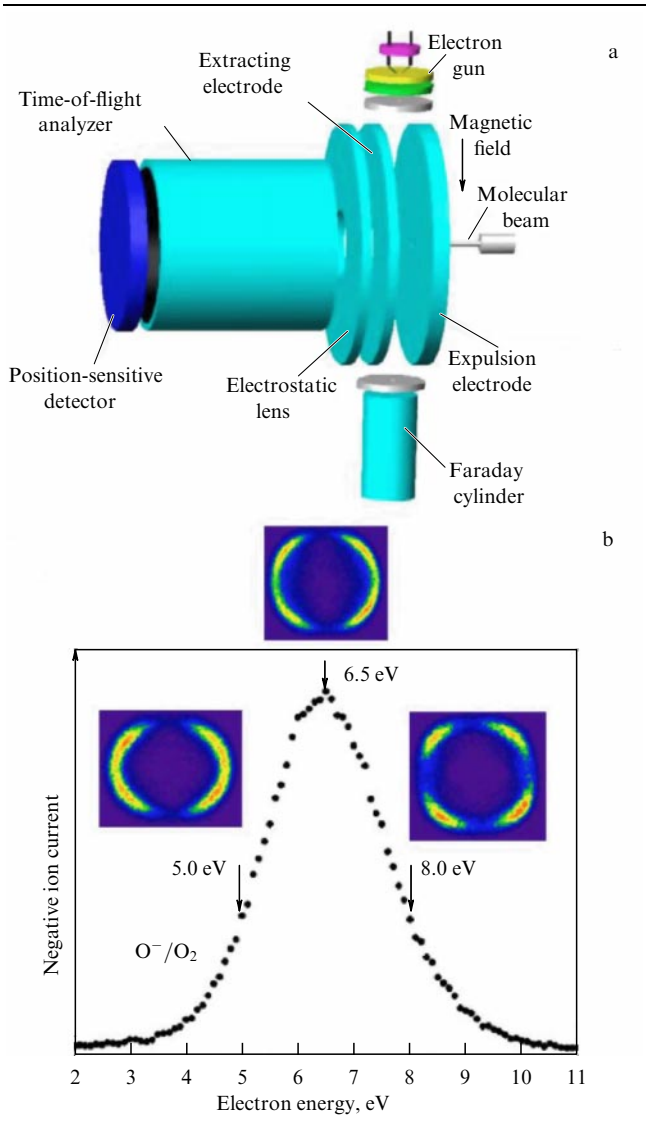

Figure 2. (Color online.) (a) Velocity slice imaging technique; (b) current of O^- anions produced after the capture of electrons by O_2 molecules as a function of electron energy; velocity slices recorded at three indicated energies; the electron beam is directed in images from top to bottom. (Adapted from [94].)

The application of this technique for DEA studies requires solving several technical problems [30]. For example, the electric field in the interaction region should not affect the electron beam, which requires the use of a pulsed regime, while the influence of secondary electrons is suppressed by a certain configuration of a magnetic field. A position-sensitive detector can be constructed based on microchannel plates and fast electronics for determining the NI incidence place [96, 97]. A more accessible variant is the use of a phosphorescence screen and data accumulation with a charge-coupled device (CCD). The required time resolution is achieved by the fast (~ 1 ns) switching of a microchannel plate. The delay between the electron beam pulse and the microchannel plate switching is determined by the NI time of flight in the drift region. Beginning with Krishnakmar's pioneering work, the method was widely applied for DEA studies at laboratories in Mumbai and Calcutta (India) [98], Milton Keynes (Great Britain) [99, 100], Heidelberg (Germany) [101], Berkeley (USA) [97, 101], Auburn (Alabama, USA) [102], and China [103–105]. It is assumed in [29] that this method can be accepted in the next decade as a standard instrument for DEA analysis.

2.3 Polarized electrons and detection of neutral fragments

The use of spin-polarized electrons in an irradiating beam [106, 107] allows one to distinguish differences in the DEA spectra of enantiomers and to study electron-induced effects in chiral molecules [108]. In these papers, the DEA was studied for camphor molecules containing halogen atoms, which are detached most efficiently in the form of NIs. It was shown in [106, 107] that the detachment efficiency of the halogen NI for a given enantiomer depends on the polarization of the primary electron beam. These studies are closely related to the Wester–Ulbricht hypothesis [46, 109] and require the development of methods for obtaining polarized electrons [110].

Until recently, the structure of neutral fragments produced due to DEA was determined based on the energy balance and most probable bond dissociations in target molecules. Quantum chemistry methods (see Section 3.4) allow one to calculate the DEA energetics, thereby predicting the structure of neutral fragments even in the absence of thermochemical data. The detection of neutral fragments by their electron-impact ionization immediately after NI detection was developed in [111]. The authors managed to measure directly the yield of dechlorinated radicals produced due to electron capture by CCl_4 molecules [111].

2.4 Mass analyzer based on a sector magnetic field and a quadrupole filter

We will describe briefly the experimental setup in Ufa [19] schematically shown in Fig. 3. This construction does not implement the crossed bean method, because the electron-molecule interaction occurs in an ionization chamber. An electron beam with a specified energy is collimated by a longitudinal magnetic field and is transmitted through vapor of the matter under study. The currents of NIs mass separated in a sector magnetic field (the resolving power was 1100, the interval of mass number was 2–700, and the acceleration voltage was 4 kV) were detected as functions of electron energy in the range of 0–15 eV. The electron energy spread estimated from the SF_6^- ion current was 0.4 eV for a beam current of 1 μA. The accuracy of measuring the resonance peak positions was ±0.1 eV. The electron energy scale was

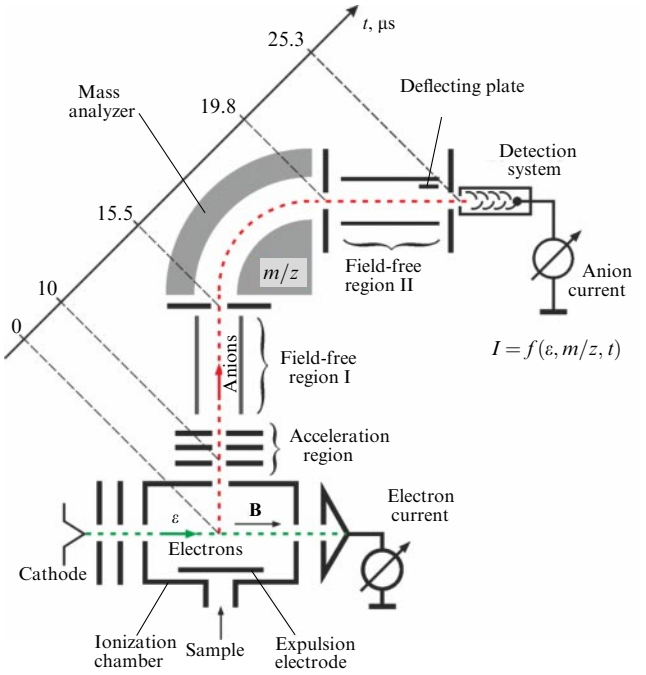

Figure 3. (Color online.) Schematic of the DEA spectroscopy technique using a sector magnetic field as a mass analyzer. Indicated are characteristic flight times of SF_6^- ($m/z = 146$) from the moment of ion appearance in the ionization chamber to its detection with a secondary-electron multiplier.

calibrated by the current of SF_6^- anions produced by the capture of thermal electrons by SF_6 molecules and also NH_2^- from NH_3 (the resonance at 5.65 eV) and O^- from CO_2 (maxima at 4.4 and 8.2 eV).

The high measurement sensitivity ensures the detection of metastable NIs (Section 3.5). Measurements of the mean autodetachment time $\langle \tau_a \rangle$ of electrons from MNIs proposed for time-of-flight analyzers [112] are performed by applying a high voltage (2 kV) to a deflecting plate (see Fig. 3), which ensures the detection of a signal only from neutral particles produced due to electron autodetachment in region II without a field. The value of $\langle \tau_a \rangle$ is determined from the ratio of this signal to the total signal [19] (Sections 3.6 and 4.4).

Note that at present the crossed beam technique uses mainly DEA spectrometers equipped with a quadrupole mass analyzer [113–117] and a trochoidal monochromator [22]. This reduces the electron energy spread to 30–50 meV for beam currents of the order of a nanoampere, as in the Bratislava experiment [118]. The electron and molecular beams interact in a small region of their crossing, which, along with the use of a monochromator, considerably reduces NI currents. Another disadvantage of such instruments is that they cannot be applied for detecting metastable ions and direct measuring of $\langle \tau_a \rangle$ because of the use of a low accelerating voltage (~ 400 V). However, combined measurements performed with instruments having considerably different timescales and sensitivities can provide additional information on the evolution of MNIs (Section 3.5).

Figures 4 and 5 show the results of DEA studies with rhodanine molecules [119, 120] performed in Ufa as well as by the method of electron transmission spectroscopy [121]. This technique [7, 8] is used to measure the energy of resonances in the total scattering cross section by detecting the first energy derivative of the electron current ($dI_{el}/d\varepsilon$ in Fig. 4) trans-

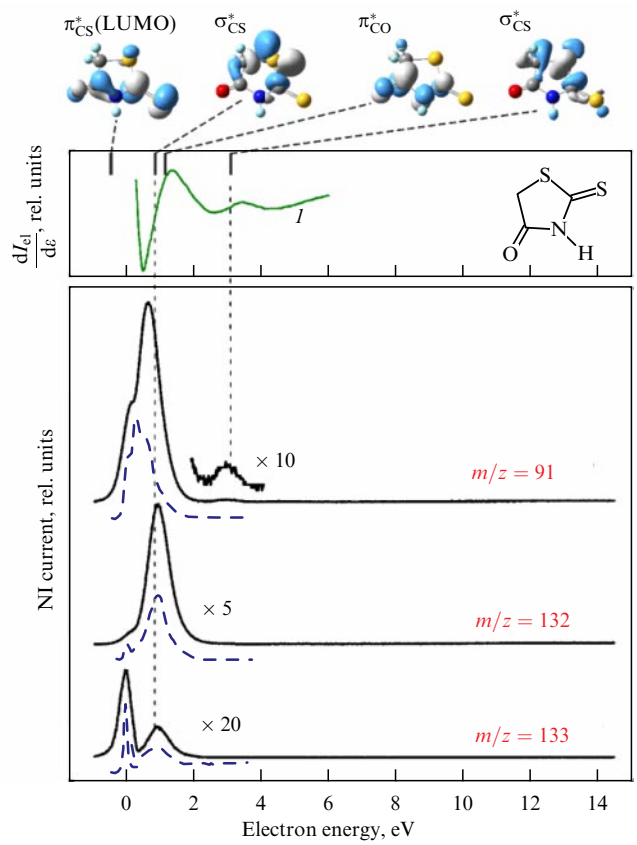

Figure 4. (Color online.) Currents of most intense NIs in the rhodanine mass spectrum as functions of electron energy; a correspondence is shown between maxima of NI currents and shape resonances recorded in the spectrum of transmitted electrons (green curve *1*) at energies of 0.84 and 3.08 eV and positions of the low-lying vacant orbitals of a rhodanine molecule [119].

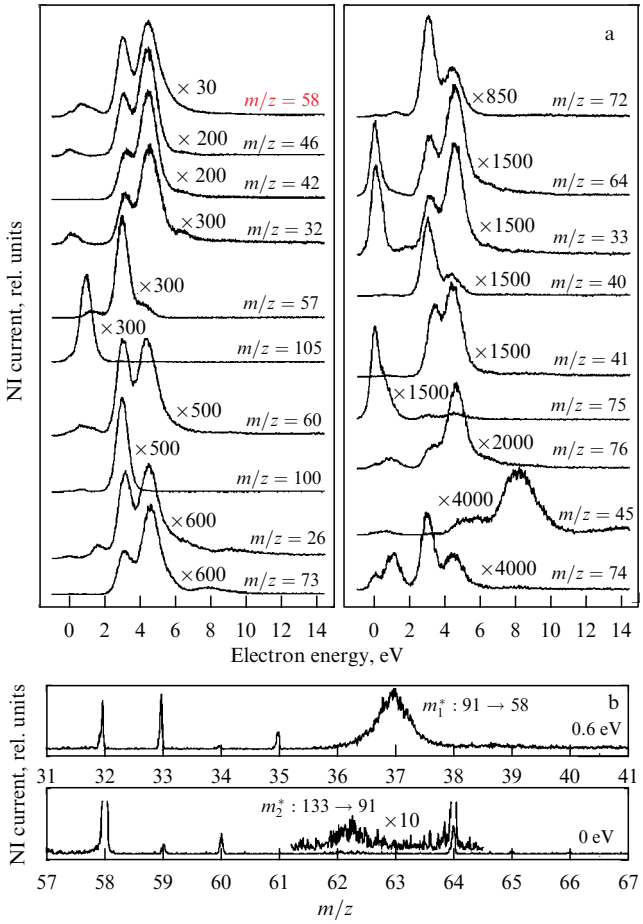

Figure 5. (Color online.) (a) Currents of less intense NIs in the rhodanine mass spectrum as functions of electron energy; structures of fragments shown in red ($m/z = 58$) here and in Fig. 4 are presented in Fig. 6; the rest are in paper [120]; (b) broad mass peaks m_1^* and m_2^* recorded at fixed electron energies (0.6 eV and thermal) indicate slow (microsecond) successive MNI decays.

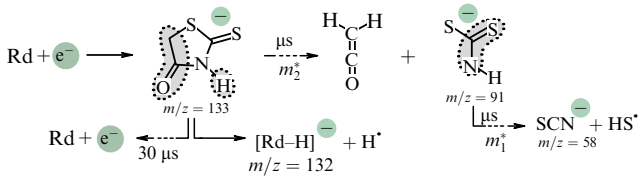

Figure 6. Main decays of rhodanine (Rd) MNIs upon trapping of thermal electrons on lower vacant orbital π^*_{CS} (see Fig. 4) by the Feshbach vibrational resonance mechanism; grey regions indicate structural elements detached in the form of neutral particles of NIs; m_1^* and m_2^* are slow (microsecond) decays (see Fig. 5).

mitted through the ionization chamber without collisions between the electrons and molecules under study. High-resolution DEA spectra (blue dashed curves in Fig. 4) exhibit narrow peaks in the cross-section dependence on the electron energy. However, only the most intense signals are detected: long-lived MNIs ($m/z = 133$) and fragmented NIs ($m/z = 132$ and 91) corresponding to the ejection of a hydrogen atom and the opening of a cycle with the detachment of a neutral CH_2CO molecule, respectively. High-sensitivity experiments reveal numerous less intense MNI decompositions (black curves in Figs 4 and 5), metastable NIs (Section 3.5) (see Fig. 5), and can be used to estimate $\langle\tau_a\rangle$, considerably supplementing the picture of fragmentation of rhodanine molecules during thermal electron capturing (Fig. 6).

2.5 Molecular-beam formation methods

The required concentration of molecules under study in the region of interaction with electrons is produced, as a rule, by thermal evaporation at temperatures not exceeding 200–300 °C [14, 15, 19, 121, 122] with the characteristic degree of excitation of vibrational-rotational states of a few tenths of an eV. Crossed-beam experiments use an effusive molecular beam containing molecules with a known amount of vibrational energy [123]. This makes possible studying rather drastic temperature effects both in the DEA cross section [124] and in the detection of long-lived (microseconds) MNIs [125]. The high vibrational states of target molecules can be populated with the help of a second electron beam [126]; however, this technique has not been widely accepted. Additional possibilities are presented by optical pumping of vibrational degrees of freedom [127] and the preparation of excited electronic states of initial molecules [84, 85, 128], which not only allows studying the evolution of MNIs with a specified amount of internal energy but also finds practical application [129]. Studies of electron capture by excited molecules are presented in review [130].

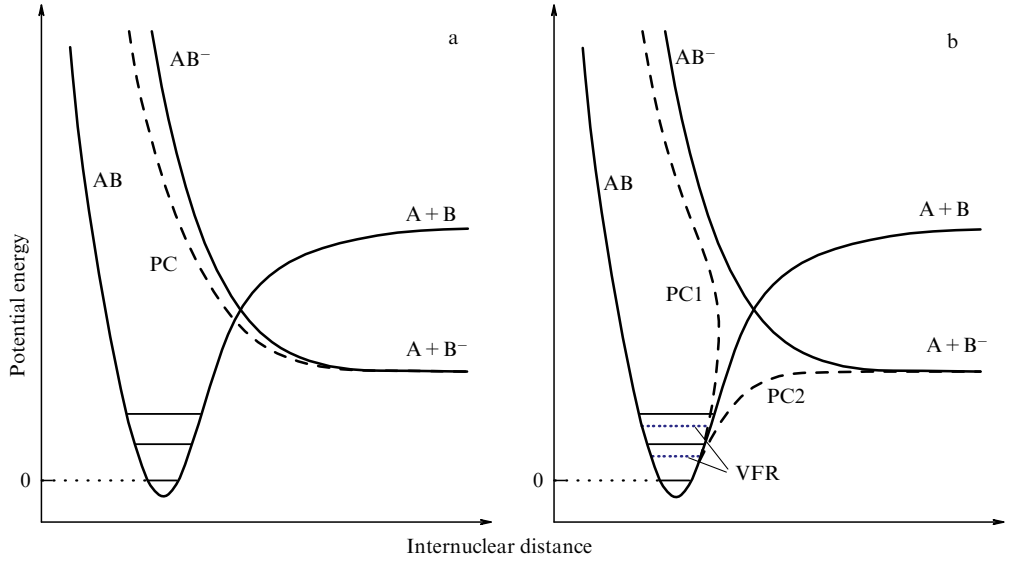

Figure 7. (Color online.) (a) In the absence of long-range interaction: AB is the term of a neutral molecule (plus an electron at infinity); AB^- is the term of a negative ion (dashed curve corresponds to one resonance state (RS) slightly stabilized due to interaction with a continuum). (b) In the presence of a dipole or polarization interaction: RS1 and RS2 are diabatic terms appearing due to the presence of a weakly bound NI state; quasi-bound vibrational RS2 terms located at positive energies lead to the formation of VFRs. (Adapted from [25].)

3. Theoretical and calculation methods. Interpretation of experimental results

3.1 Long-range interaction effects in resonance electron scattering and nonvalent states of negative ions

The long-range interaction of electrons with molecules gives rise to dipole-bound states (DBSs) [131, 132]. The mixing of these states with valent states can be accompanied by the redistribution of the excess energy over the internal degrees of freedom [133, 134]. This results in the formation of long-lived NMIs or in dissociation [135, 136], while DBSs themselves are treated as weakly bound (hundreds of meV) doorway states [137, 138]. Nonvalent NI states are important in the presence of environment and determine electronic processes in liquefied gases, reactions in the interstellar medium, and radiation-induced DNA damage [139, 140], which requires the extrapolation of gas-phase results to processes in the medium [141–144]. A few observations of quadrupole-bound NIs [145, 146] give estimates of the bond energy in the area of a few to tens of meV.

As shown in review [147], the suppression of long-range effects in the presence of a condensed environment does not necessarily reduce the DEA cross section, but can increase it [148, 149], which is a key element in using the results of gas-phase experiments to describe biochemical processes (see Section 4.2 below). For example, the DEA cross section (detachment of a chlorine anion) for CH_3Cl molecules adsorbed on a Kr surface is five orders of magnitude higher than the one in the gas phase [150]. This is explained by the increase in the survival factor [12] leading to a drastic decrease in the autodetachment probability in a condensed state due to stabilization of NIs during their interaction with the surface [151–153].

Because DBSs are mainly determined by polarization effects, the author of review [147] points out some incorrect considerations, assuming the existence of a critical dipole moment equal to 1.625 D [154], which is necessary for DBS formation. It is more correct to speak about 'weakly bound' or 'diffusion' NIs, without specifying the forces responsible for the bond appearance, because the bond energy is determined by both long-range and short-range interactions [155]. Long-range effects can be taken into account in the R-matrix theory [156, 157], which is the expansion of the modified effective range theory [158] and allows one to describe resonance scattering using the Breit–Wigner formula [159]. The successes of the theory in the description of long-range effects upon resonance scattering achieved in the two last decades are presented in detail in [147].

The long-range interaction gives rise to vibrational Feshbach resonances (VFRs) [25, 147], as shown in Fig. 7. We assume that in the absence of long-range interaction only one resonance state (RS) exists — the adiabatic term shown by the dashed curve in Fig. 7a. Vibrational levels of a weakly bound state, shown by blue dotted lines, lie lower than vibrational levels of a neutral molecule by the value of the bond energy (Fig. 7b, the diabatic RS2 term). The zero vibrational level of such a composite state [25] can lie in a bound region, which corresponds to a stable NI not observed in the scattering of free electrons. Vibrational levels of a composite state lying in a continuum (in an unbound region with positive energies) correspond to the formation of VFRs. Their decay by autodetachment is possible due to kinetic mixing of two resonance states and a continuum and is manifested as narrow peaks observed below the threshold of vibrational excitation of target molecules in the cross sections of elastic scattering or vibrational excitation. Observations of VFRs for molecules with dipole moments below the critical value and even nonpolar molecules [147] confirm that the polarization interaction is sufficient for DBS formation.

Vibrational Feshbach resonances are observed in the cross section of hydrogen detachment from uracil and thymine molecules [135, 160, 161]. The dipole moment of uracil (4.7 D [162]) considerably exceeds the critical value, i.e., the main contribution is expected from the dipole interaction. However, the structure of these molecules is too complex to use the nonlocal resonance theory, and therefore the

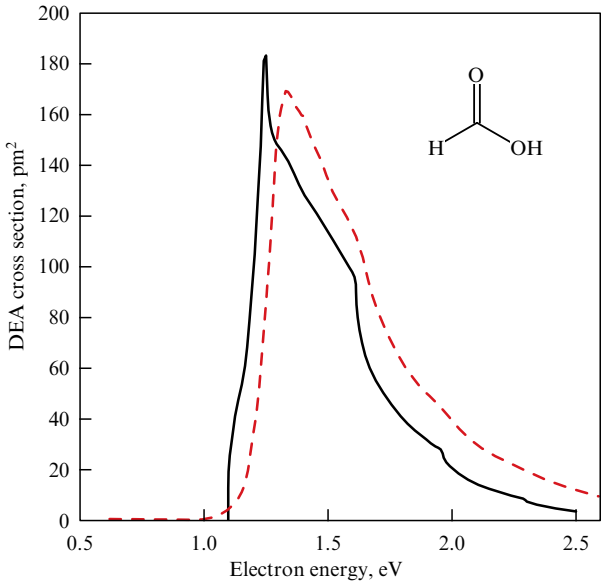

Figure 8. Comparison of experimental (red dashed curve) [165] and calculated (black solid curve) [166] ejection cross section for a hydrogen atom ejected from a negative ion of formic acid due to O–H bond dissociation. (Adapted from [147].)

pseudodiatomic approximation is used with a separated reaction coordinate (the N–H bond). The rest of the degrees of freedom are treated as a 'frozen frame', which results in an adequate description of the detachment of a hydrogen atom from a uracil MNI below the excitation threshold of the N–H bond vibrations [163, 164]. The measured cross section for $[M-H]^-$ ion formation from formic acid (the dipole moment is 1.42 D [167] and is lower than critical) well agrees with the theoretical prediction (Fig. 8). An analytic approach allows narrow resonances (~ 0.1 eV) to be described in the spectra of transmitted electrons of five-membered heterocyclic compounds (imidazole, pyrazole, and pyrrole) detected lower than the energy of the first shape resonance (SR) [168], as shown in Fig. 9. According to calculations [168], these spectral features are caused by symmetry-allowed DBS mixing with a valence state associated with the low-lying σ^*_{N-H} MO and are not observed for isoxazole molecules not containing the N–H bond.

The formation of nonvalent NIs is also studied by time-resolved photoelectron spectroscopy [134], which allows one to determine the nature of the initial state and evolution times. Correlation forces can be sufficient for electron holding in correlation-bound NIs [169, 170], which are intermediate in the formation of valence states. For example, it was shown in [171] that the electron transfer from an iodine NI to a hexafluorobenzene molecule upon photoexcitation of the $I-C_6F_6$ cluster results in the relaxation of the initial correlation-bound NI to a valence state at the femtosecond timescale [172, 173]. An example of the reverse process is the ultrafast conversion of the excited valent NI of p-Coumaric acid to a DBS [174].

3.2 *Ab initio* methods applied to resonance scattering problems

The nonlocal resonance theory [175] quite accurately characterizes the electron-molecule interaction, but mainly for diatomic molecules or in the pseudodiatomic approximation, whereas the local approximation [176] does not

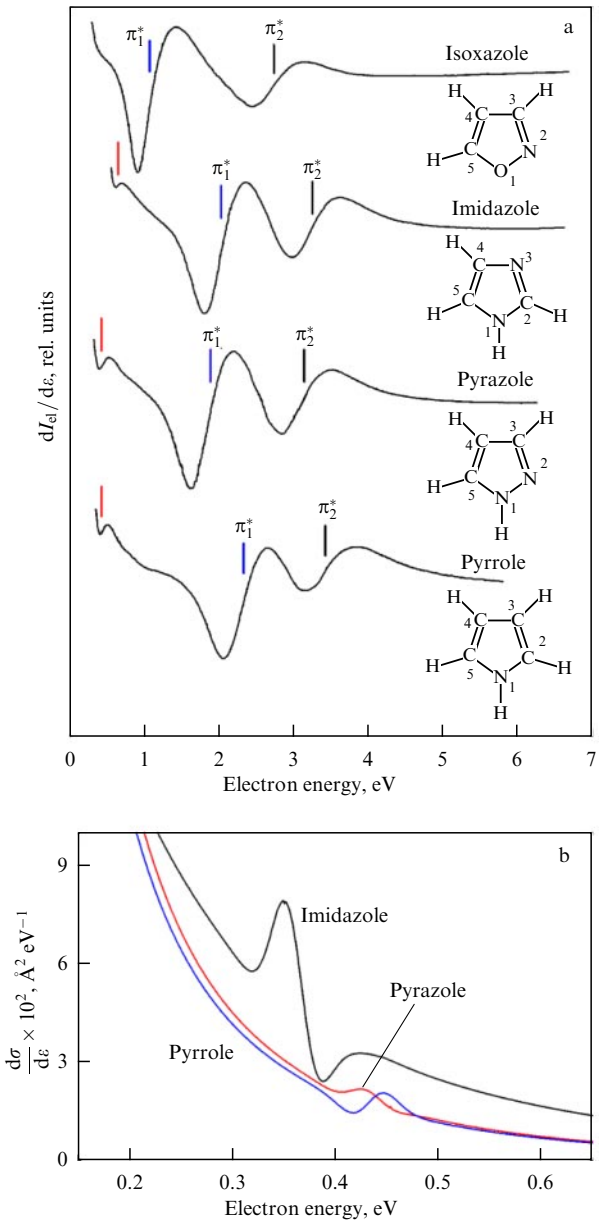

Figure 9. (Color online.) (a) Narrow features near 0.45 eV (red bars) in spectra of transmitted electrons of imidazole, pyrazole, and pyrrole; first shape resonances (electron trapping on the lower vacant π_1^*-MO) located at energies of 1.90, 1.87, and 2.33 eV, respectively (blue bars); (b) calculated dependence of first derivative of scattering cross section on electron energy explaining the observation of resonances at low energies [168].

describe threshold phenomena. An appropriate choice is the R-matrix method [27, 156, 177], which is analogous to the nonlocal theory of the complex potential and can explain many features of DEA cross sections (behavior at low collision energies, resonances, and temperature effects), but can be applied only to rather simple structures, for example, glycine and formic acid [166]. Good agreement between theory and experiment was achieved for hydrohalogens. However, difficulties are encountered even for the simplest F_2 and Cl_2 molecules [27].

The R-matrix method can be applied using the program package [178, 179] to calculate diffusion NIs and differential and transport scattering cross sections. A simple method for estimating the DEA cross section based on the calculation of the formation cross sections of resonance states and survival

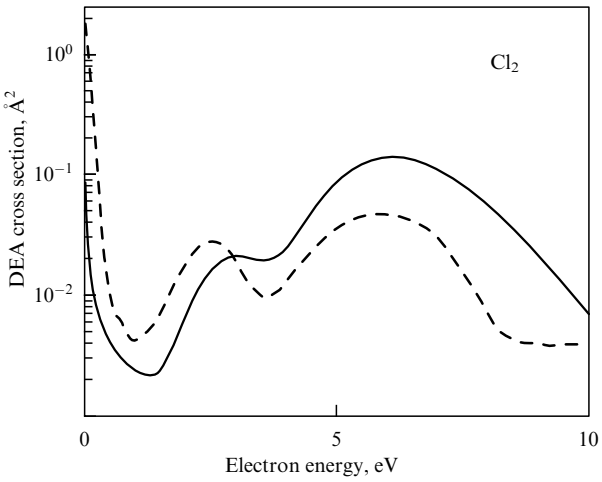

Figure 10. DEA cross section for Cl_2 molecules measured as a function of electron energy [181] (dashed curve) and calculated using the Quantemol-N program package [178] (solid curve). (Adapted from [180].)

factors [180] adequately describes experimental results for simple molecules (Fig. 10). The use of more specialized programs [182] is described in review [183]. Along with the R-matrix method, a number of theoretical approaches exist describing electron-molecular scattering [184, 185], including methods based on the variational principle of Kohn [186] and Schwinger [187]. A description of the latter technique and examples of calculations of DEA cross sections and integrated cross sections for uracil halogen derivatives are presented in [188].

3.3 Simulation of dissociation of negative ions by molecular dynamics methods

Molecular dynamics methods do not describe electron autodetachment but can be applied for simulations of the final DEA stages, realized in a program package [189, 190] for describing the monomolecular decomposition of ions using statistical approximation [191]. The modern theory allows the expansion of the typical timescale (5–10 ps) up to nanoseconds; however, the microsecond interval corresponding to metastable decays in mass-spectrometer experiments [192, 193] remains inaccessible. The program package was used to determine the relative intensities of fragments and characteristic reaction times for derivatives of acetonitrile and cyanamide in the attachment of electrons with energies of 0–20 eV [194]. This model assumes (Section 3.6) the relaxation of MNIs to the ground electronic state and the intramolecular redistribution of the internal energy, which is typical of structures with a positive electron affinity exceeding 0.5 eV [193]. The MNI dynamics can be studied using hybrid functionals in the DFT in combination with *ab initio* molecular-dynamics methods, for example, for predicting the observed bond dissociations in nucleotides [195] and also complex rearrangement of atoms in the MNIs of fluoroderivatives of toluene, aniline, and phenol [196]. It was shown in [197, 198] that the C–Cl bond dissociation time in an anion during the DEA by chlroalkylbenzene molecules of the type $C_6H_5(CH_2)_nCl$, $n = 0-4$ [199] was tens of femtoseconds and nonmonotonically dependent on the length of the alkyl substitute.

The electron-induced decomposition of chloroethane was studied in [200] based on a mixed quantum-classical approach [201] taking into account all the vibrational degrees of freedom of target molecules, unlike previous studies [202, 203]. The energy of resonances was calculated by methods convenient for calculating valent bound NI states and their widths — using a combination of calculations of bound states and the scattering theory. It was shown in [200] that electron autodetachment occurs for about 10 fs, and its attachment on the σ MO by the SR mechanism leads to the rapid stabilization of MNIs due to the change in the C–Cl bond length. The temperature dependence, value, and shape of the formation cross section of Cl^- were predicted. These methods can simulate the DEA in the presence of an environment, for example, solvation effects were found at the final stage of the electron-induced dissociation of thymine molecules [204].

3.4 Quantum-chemical estimates of the shape resonance position and fragment appearance thresholds

Modern program packages [205, 206] allow estimating the molecular properties required to interpret DEA spectra whose resonance character in the energy region below the first electronic excitation ($\lesssim$4 eV) is determined by the electron vertical attachment energy (VAE) [7, 8, 12]. The VAE values can be estimated by calculating the energy of vacant MOs (VOE, Virtual Orbital Energy) by the Hartree–Fock (HF) or DFT methods using the hybrid B3LYP functional and the standard basis set 6-31G(d), despite the fact that NI calculations involve difficulties [207] that do not appear in calculations of positive ions or neutral molecules. However, a linear correlation [199, 207–209] exists between experimental VAEs [210, 211] and the VOE of neutral molecules calculated in bases not containing diffusion functions. The empirically determined parameters of this linear relation depend on the type of MO (σ^* or π^*) and lead to more accurate estimates for molecules with close structures.

The relation $\mathrm{VAE} = 0.8054 \times \mathrm{VOE} + 1.2110$ was obtained by calculations using the B3LYP/6-31G(d) method for compounds having π^* MOs, including heteroaromatic hydrocarbons [199], while the relation $\mathrm{VAE} = (\mathrm{VOE} - 2.12)/1.87$ was obtained using the HF/6-31G(d) method used for the π^* MOs of chloroderivatives of salicylic acid [212]. The energy of σ^*_{C-Cl} orbitals is scaled by the expression $\mathrm{VAE} = 0.8111 \times \mathrm{VOE} + 1.6097$ obtained by the B3LYP method for chloroderivatives of alkanes [213] or by the expression $\mathrm{VAE} = (\mathrm{VOE} - 2.83)/1.11$ obtained by the HF method [214]. Note that SRs related to electron attachment on the σ^*-MO are short-lived and are more weakly manifested in spectra than π^*-resonances. For this reason, the values of σ^*-VAEs obtained by this method are usually less accurate than π^*-VAEs [32].

In addition to the energy scaling of the lower vacant MO, the first vertical electron affinity (EA_v) can be calculated from the difference between the total energies of the ground state of a neutral molecule and MNI in the optimal molecular geometry, for example, in the 6-31+G(d) basis tested in [192, 199]. The adiabatic electron affinity (EA_a) can be estimated from the difference between the total energies of the ground states of a neutral molecule and MNI calculated in their optimal geometry. In the choice of large basis sets, the probability increases that single occupied MOs will be represented by a diffusion function that does not have the physical meaning [199, 208, 215]. The structures of fragment NIs and neutral fragments are determined by calculating the thermodynamic thresholds of their formation as the difference between the total energies of the ground state of a neutral

molecule and the total energy of decay products. These calculations showed that the B3LYP-6-31+G(d) method is convenient for performing such estimates [119, 120].

3.5 Kinetic decay equation for molecular negative ions

The formation of MNIs and fragmentation ions in DEA spectroscopy is described by the first-order kinetic equations, while the observed relative intensities of NI currents depend on the time window of the experiment. The extraction time of NIs from an ionization chamber (see Fig. 3) depends on the pushing and pulling potentials, as a rule, amounting to fractions of volt, and is estimated as 10 μs for SF_6^- ions [19, 193]. After acceleration, NIs subsequently pass through field-free region I, the mass-selection region, and field-free region II, and reach a detection system. The flight through each of the regions I and II for SF_6^- ions takes about 5.5 μs, and inside an analyzing magnet, 4 μs, i.e., the time between the moments of formation of SF_6^- ions and their detection is about 25 μs.

During the flight, MNIs can either lose an excess electron or dissociate, which is described by the first-order kinetic equations

$$M^-(t) = M_0^- \exp\left[-(k_a + k_d)t\right], \quad (1)$$

$$R^-(t) = M_0^- \frac{k_d}{k_a + k_d}\left[1 - \exp\left[-(k_a + k_d)t\right]\right], \quad (2)$$

where M_0^- is the number of molecular ions at the formation moment ($t = 0$), k_a and k_d are the rate constants for autodetachment and dissociation, and $R^-(t)$ and $M^-(t)$ are the numbers of fragmentation ions and MNIs at the moment t. All the fragmentation ions produced in the ionization chamber are detected as 'normal' narrow mass peaks corresponding to the integer mass numbers. If an NI is decomposed in the reaction $M^- \to m^- +$ *a neutral fragment* after escape from the ionization chamber, i.e., in the region of action of an accelerating potential or in field-free region I, it is detected as a broad metastable peak with the apparent mass m^* (Fig. 5b), which can be calculated as [216, 217]

$$m^* = \frac{m^2}{M}. \quad (3)$$

Metastable peaks show that M^- was decomposed at the microsecond timescale.

Expressions (1) and (2) estimating the numbers of MNIs and fragmentation anions can explain [218] the difference between their relative intensities, which is detected with instruments with different time windows using a sector magnetic analyzer (see Fig. 3) and a quadrupole mass filter with the extraction and flight times equal to 20 and 200 μs, respectively. The DEA spectra of bromobiphenyl [219] obtained using instruments with different time parameters are considerably different, but the approach described above allows one to reconcile the results of experiments, thereby removing the problem of their reproducibility.

3.6 Statistical approach for describing electron autodetachment

Dissociative electron attachment by polyatomic molecules is a multistage process [19] including electron capture by a molecule with the formation of a metastable MNI followed by its evolution, which assumes transitions to other rovibronic states with possible energy losses by emission, autodetachment, and dissociation. These competing processes are characterized by decay constants, which give information on the mechanism of redistribution of the excess energy in the MNI. Note that the DEA can be treated as a multistage process only when the lifetime of a molecule + electron complex exceeds the electron flight time over a distance equal to the effective diameter of the molecule.[1] Only in this case the electron attachment have the resonance character; it is governed by the VFR mechanism at thermal energies and by the SR mechanism or the electronically excited resonance (EER) mechanism [19] at epithermal energies. During radiative attachment, an electron moves to a bound state due to radiative energy losses, which is possible for any collision energy. Despite the absence of experimental data, theoretical estimates show in [222] that radiative attachment cross sections are negligibly small, i.e., the evolution of MNIs is determined by the excess energy, equal to

$$E_{exc} = E_{vib} + \Delta + E_{rot} + EA_a + \varepsilon, \quad (4)$$

where E_{vib} is the vibrational energy (above the zero-vibration energy) of a target molecule, Δ is the difference between zero-vibration energies of the target molecule and MNI, E_{rot} is the initial rotational energy of the target molecule, and ε is the incident electron energy. The redistribution of E_{exc} over rovibronic degrees of freedom of MNIs determines all the variety of evolution processes having a statistical nature.

Electron autodetachment plays a key role in the understanding of DEA processes, while a knowledge of the corresponding decay constant allows one to distinguish 'slow' statistical decay processes from 'fast' dynamic processes [223]. Unfortunately, DEA spectroscopy cannot be used to simultaneously measure the decay constants of dissociation and autodetachment, and only the total MNI decay constant can be measured. Nevertheless, autodetachment processes can be studied in a 'pure' form when dissociation is impossible due to a lack of energy, which is usually observed in the thermal and near epithermal electron energy region ($\sim 0-2$ eV). Namely such processes will be considered below.

The MNI decay constant k_a in the case of autodetachment is related to the measured lifetime τ_a by the expression $k_a = 1/\tau_a$. Assuming that MNIs decay exponentially and are physically indistinguishable, choosing any convenient 'time window' $\Delta t = t_1 - t_2$ in the MNI trajectory, and measuring the ratio I_i/I_n of the charged and neutral components, the required τ_a can be found from the expression

$$\tau_a = \frac{\Delta t}{\ln(1 + I_n/I_i)}. \quad (5)$$

Obviously, in the case of exponential decay, τ_a is independent of the time boundaries t_1 and t_2 and the size Δt of the time window.

[1] This is not always the case. For example, for the DEA by H_2 molecules, the lifetime of the bound state is comparable to the electron free path time over a distance equal to the H_2 molecule diameter [220]. This is the so-called direct DEA process without the formation of an intermediate long-lived complex. Such direct processes are calculated using the quantum scattering theory in a system of several particles [221].

Table. Experimental values of MNI lifetimes (time-window boundaries for static and time-of-flight mass spectrometers are presented at the accelerating voltage of 4 kV).

MNI	τ_a, μs	Reference	Mass spectrometer type	Time-window boundaries, μs	
				Lower	Top
SF_6^-	150	[236]	MI-1201 static mass spectrometer	24	30
	10	[112]	Specially constructed time-of-flight mass spectrometer	~ 1	6
	25	[223]	Bendix, Model 14-206 time-of-flight mass spectrometer	~ 1	9
	25.8	[244]	Bendix, Model 14-206 time-of-flight mass spectrometer	~ 1	9
	32	[245]	Bendix, Model 14-206 time-of-flight mass spectrometer	~ 1	9
	70	[226]	Bendix, Model 3015 mass spectrometer	~ 1	28
	68	[227]	Bendix, Model 3015 mass spectrometer	~ 1	28
	67	[246]	Bendix, Model 3015 mass spectrometer	~ 1	28
	500	[247]	ITsR mass spectrometer	~ 1	~ 1000
	$50-10^4$	[229]	ITsR mass spectrometer	~ 1	$\sim 10^4$
$C_6H_5NO_2^-$	90	[236]	MI-1201 static mass spectrometer	22.5	27.5
	47.3	[227]	Bendix, Model 3015 mass spectrometer	~ 1	25.6
	17.5	[224]	Bendix, Model 14-206 time-of-flight mass spectrometer	~ 1	8.1
$C_6F_6^-$	35	[236]	MI-1201 static mass spectrometer	27.2	33.9
	12	[248]	Bendix, Model 14-206 time-of-flight mass spectrometer	~ 1	10

As experimental data were gradually accumulated, it became clear 'that something was wrong' with the exponential decay law for MNIs. SF_6 molecules, widely used as a reference in measurements of τ_a, produce long-lived MNIs SF_6^- at an electron energy close to zero, and the measured values of τ_a significantly differ from each other (see Table). The almost three-order-of-magnitude spread in the values of τ_a for the exponential MNI decay cannot be explained by the focusing of neutral and charged particles, conditions in the ion source (temperature, pressure, electron energy distribution), and the detection efficiency [112, 224–227]. These factors can cause systematic errors in measuring τ_a with different instruments; however, the great value of this error (up to 1000%) stimulated a search for other reasons for this error. The authors of [226, 227], citing paper [228], assume that the large spread in measuring τ_a can be explained by the quasi-equilibrium theory (QET) [225], which predicts that, even in the case of the capture of monoenergetic electrons, the initial thermal distribution of target molecules leads to the production of MNIs with different excess energies and therefore with different τ_a. Thus, their decay should be nonexponential, and τ_a will depend on the time window and ionization chamber temperature.

The nonexponential decay of SF_6^- was observed for the first time in experiments with an ion cyclotron resonance (ICR) mass spectrometer [229]. Depending on the observation time, τ_a changed from 50 μs to 10 ms. Similar results were obtained for SF_6^- and $C_6F_6^-$ during the transfer of Rydberg electrons [230, 231] in experiments with electrostatic circular storage [232] and with a static mass spectrometer for *o*-carboran-12 [233], which confirms in fact the hypothesis [228] about the necessity of taking into account the energy distribution of target molecules within the framework of the QET [225, 228] and the static RRKM (Rice–Ramsperger–Kassel–Marcus) theory [234, 235]. In the case of nonexponential decay, the quantity τ_a, measured by the Edelson–Khvostenko method [19, 112], is not a characteristic MNI itself but reflects the evolution of a statistical ensemble, being the average $\langle\tau_a\rangle$. Theoretical approach [249] gives the dependence of τ_a on the incident electron energy, but ignores the temperature dependence. Model [5] describes τ_a for different vibrational states of a target molecule at extremely high temperatures, when nuclear vibrations can be assumed classical. The values of $\langle\tau_a\rangle$ can be estimated using a one-dimensional statistical model [250, 251]. However, quantitative agreement is achieved only at energies above the MNI observation maximum.

The parameters of molecules and electrons interacting with them determining $\langle\tau_a\rangle$ can be conventionally separated into individual and collective. The former include the electron affinity, the attachment cross section, vibrational frequencies, the number of active degrees of freedom of a molecule, and the electron energy. The latter characteristics of a statistical ensemble are temperature, the vibrational energy, and kinetic energy distributions of target molecules. The values of $\langle\tau_a\rangle$ are estimated in these models by using in fact the average values of collective parameters as individual. In this case, $\langle\tau_a\rangle$ is independent of the time window, the spread of experimental values of $\langle\tau_a\rangle$ is difficult to explain, and dependences of $\langle\tau_a\rangle$ on temperature and the electron energy are poorly reproduced. These disadvantages are absent in models directly taking into account the distributions of molecules over vibrational states and electrons over energies.

The multiexponential decay model [236] considers MNIs distributed in groups characterized by their own τ_a and obeying an exponential decay law. The greater the size of the time window and the farther its boundaries from the electron capture moment ($t = 0$), the more long-living MNIs will be detected. During the capture of thermal electrons, i.e., the formation of VFRs [19, 237], the MNI distribution over the excess energy is determined by the distribution of molecules over vibrational states, which was found using the quantum

approximation and Boltzmann statistics. The dependence of τ_a on the vibrational excitation of molecules was obtained in the Illenberger–Smirnov–Kompaneits (ISK) model [5] in the form

$$\tau_a = \tau_0 \frac{n(R^-)}{n(R_m)}, \qquad (6)$$

where τ_0 is the characteristic variation time of the distribution over vibrational states, $n(R_m)$, and $n(R^-)$, is the number of vibrational states for the nuclear configuration responsible for the electron capture and corresponding to the maximum electron bond energy, in other words, the number of vibrational states of a molecule and MNI. The model follows from the RRKM theory [235] and is based on the Born–Oppenheimer approximation and on the assumption that the excess energy of an MNI completely transfers to its vibrational energy. Results obtained in [236], taking into account only the distributions of molecules over vibrational states, qualitatively describe the values of τ_a for SF_6^-, $C_6H_5NO_2^-$, and $C_6F_6^-$ measured with static, time-of-flight, and ICR mass spectrometers, including the dependence on temperature and the time window. Calculations performed for 9,10-anthtraquinone [238], phthalimide, pyromellitc diimide [193], and azobenzene [239] showed that the best agreement with experiments was obtained taking into account the electron energy spread as well. Figures 11 and 12 present experimental and calculated dependences for compounds forming long-lived MHIs, both in the thermal and epithermal regions of collision energies [193].

All the models existing at present and describing the electron autodetachment process confirm its statistical character and are in fact variants of the QET and RRKM for monomolecular decay reactions. Aside from expression (6) for calculating the autodetachment constant, the expression for the microscopic decay rate constant [240–242] and the Arrhenius formula [219, 243],

$$k(E_{exc}) = \frac{W^{\#}(E_{exc} - EA_a)}{h\rho(E_{exc})}, \qquad (7)$$

$$k(E_{exc}) = k_0 \exp\left(-\frac{EA_a}{k_B T_{ion}}\right) = k_0 \exp\left(\frac{NEA_a}{E_{exc}}\right), \qquad (8)$$

are used, where $W^{\#}(E_{exc} - EA_a)$ is the sum of states in an activated complex in the energy interval from zero to $E_{exc} - EA_a$, $\rho(E_{exc})$ is the energy density of MNI states, k_0 is the frequency factor, and N is the number of vibrational degrees of freedom.

Despite the obvious successes of theoretical models describing autodetachment, the contribution of radiation and rotational degrees of freedom to the redistribution of E_{exc} is still unknown. The influence of rotation is determined by the law of conservation of angular momentum for an MNI as an isolated system and by the interaction of vibrational and rotational subsystems. The rotational characteristic temperature of polyatomic molecules is fractions of degrees Kelvin. At temperatures of experiments of $\sim 360-500$ K, all three rotational degrees of freedom of a molecule are excited, and their energy $3k_BT/2$ barely changes. Later, the transfer of part of the energy E_{exc} to the rotational subsystem of the MNI depends only on the interaction with the vibrational subsystem. This interaction in the nonrigid rotator model is relatively weak [252], at least upon excitation of low ($\sim 1-3$) vibrational levels of the oscillator. At a high degree

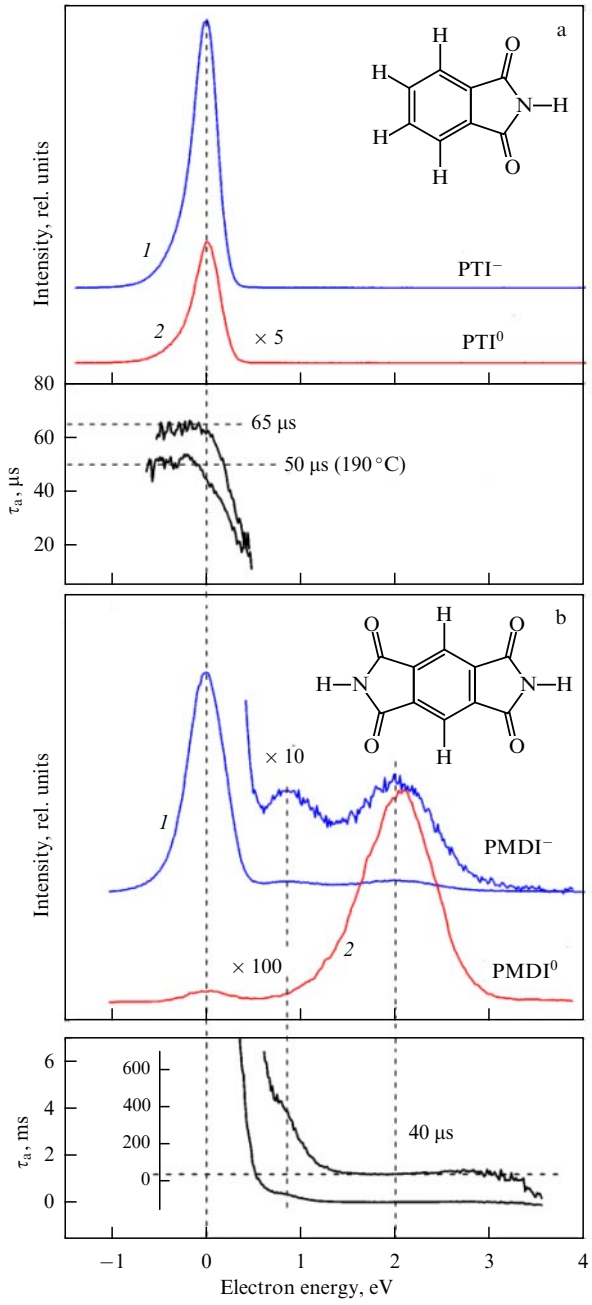

Figure 11. (Color online.) MNI currents (blue curve *1*), neutral component signal (red curve *2*), and values of $\langle\tau_a\rangle$ calculated from (5) for (a) phthalimide (PTI) at the temperature of the ionization chamber walls, 90 °C, and (b) pyromellitic diimide (PMDI) at 190 °C as functions of electron energy. Curve for $\langle\tau_a\rangle$ in PTI MNI recorded at 190 °C is also presented to compare with a similar dependence in PMDI.

of equipartition of E_{exc} among all the vibrational degrees of freedom of MNIs, this approximation should be valid for all oscillators.

The role of radiation in the redistribution of the excess energy is discussed assuming that MNIs do not emit energy during the entire time interval τ_a. Indeed, a drop in the excess energy in the form of radiation should stabilize an MNI, which would result in a drastic increase in the measured value of $\langle\tau_a\rangle$. This is not observed in experiments and is theoretically explained by small Einstein coefficients for spontaneous radiation. The mean lifetime of a state emitting a photon is

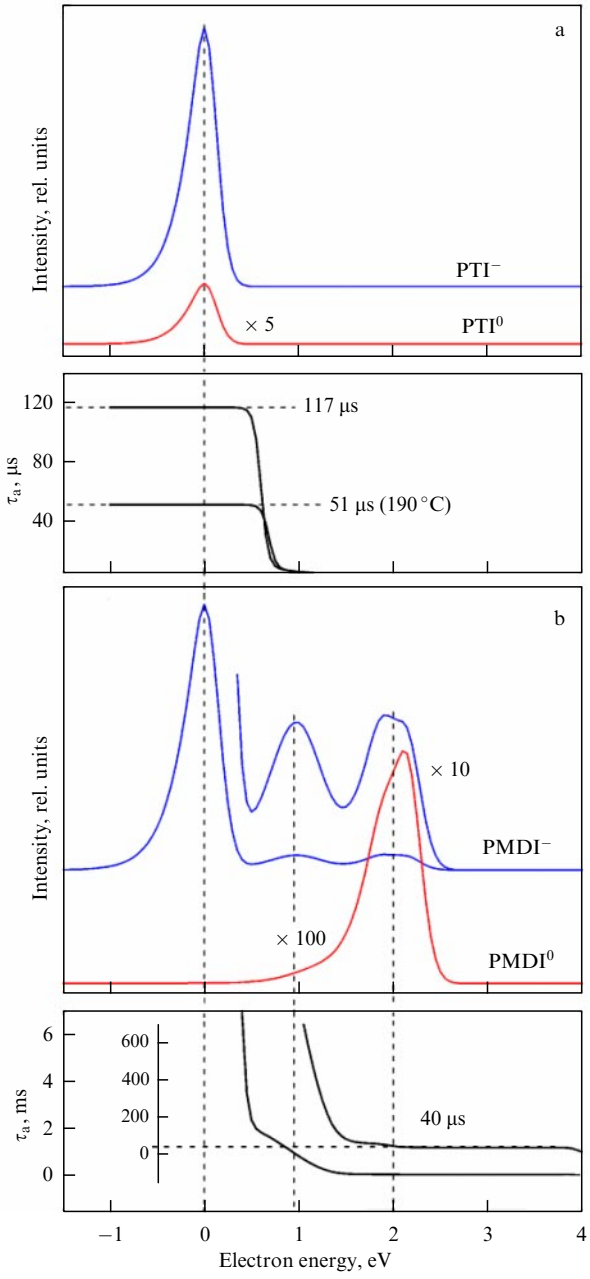

Figure 12. (Color online.) Calculated dependences demonstrating quantitative agreement with experimental results in Fig. 11 obtained in the mutiexponential model for (a) phthalimide (VFR at the thermal electron energy) and (b) pyromellitic diimide (along with VFRs, MNIs exhibit maxima at 1 and 2 eV, corresponding to shape resonances).

inversely proportional to the cube of the spontaneous transition frequency [253]. This lifetime for electronic states is of the order of 10^{-8} s and for vibrational states is of the order of 10^{-2} s. Radiative electronic transitions to the ground electronic state are important at the MNI stabilization stage. Their role is small due to competition with nonradiative transitions (see Sections 4.4 and 4.5 below), while the role of intramode vibrational transitions is small, because their lifetime lies outside the time window of the experiment [254]. Note in addition that the interaction between vibrational modes of MNIs leads to a rapid energy transfer between them at the rate of $\sim 10^{13}$ s^{-1}. This corresponds to the time of transition from one vibrational state to another equal to $\sim 10^{-13}$ s. Obviously, in this case, the excited-state lifetime of an oscillator can never reach milliseconds. The question of whether radiation can occur directly in intermode energy exchange is still open.

Note in concluding this section that the dependence of the autodetachment constant on E_{exc} according to expressions (6)–(8) is not being experimentally tested at present. The main reason is the impossibility of 'preparing' MNIs in certain vibronic states with close energies. Because of the distribution of target molecules over vibrational states and electrons over energies, the scatter in the values of E_{exc} for MNIs is in a range from a few tenths to a few eV [192, 239], whose width depends on the number of atoms in the molecule, vibrational frequencies, and temperature. In this connection, of interest are crossed-beam experiments in which a molecular beam is formed after passing through a supersonic nozzle [255, 256], i.e., almost all molecules are found in the ground electronic-vibrational state, which suppresses fragmentation and makes autodetachment a dominating decay channel of MNIs. A simultaneous decrease in the electron energy spread makes possible the experimental test of expressions (6)–(8) at energy $E_{exc} = EA_a$ and of the dependence of the thermal electron attachment cross section on the vibrational excitation value. In particular, assumption [239] about a strong dependence of this cross section on the mutual location of terms of the molecule and MNI can be confirmed by the absence of the MNI current at the thermal energy in experiments with a supersonic nozzle.

4. Some modern directions in studies of dissociative electron attachment

4.1 Mechanisms of the radiative damage of cells

The direct interaction of radiation with living tissues does not cause genotoxic effects, but results in the formation of secondary products such as ions, radicals, and electrons. The last are produced most efficiently, in the amount of about 50,000 per MeV of the incident radiation energy [257], and reach thermal equilibrium with the environment for nanoseconds. As a result, independently of the type of primary particles, regions with localized electrons with energies up to 30 eV and a distribution maximum at 9–10 eV are produced along the paths of particles. As shown in [49, 259, 260], these electrons efficiently produce damage to DNA molecules [258] and proteins [259] via the DEA mechanism. In particular, it was shown in [49] that electrons with energies from 3 to 20 eV break helices or damage the superhelical DNA structure. The dependence of the intensity of such damages on the electron energy exhibits resonances corresponding to those observed upon the DEA in the gas phase by DNA components [260]. This result initiated numerous studies (for example, [164, 261]) of the DEA by molecules simulating different types of DNA and RNA. Studies of nitrogen bases [161] opened up a broad scope of applications of the DEA results in radiation chemistry. It is shown in [154] that mechanisms of formation of the primary NI bound state [164] play an important role in the processes of damage to living tissues and the appearance of mutations.

The application of the results of DEA studies to the problems of radiation therapy has even a shorter history [262]. Radiosensibility increasing cell sensitivity to the action of ionizing radiation with the help of chemical compounds is important in radiation therapy, representing a method of

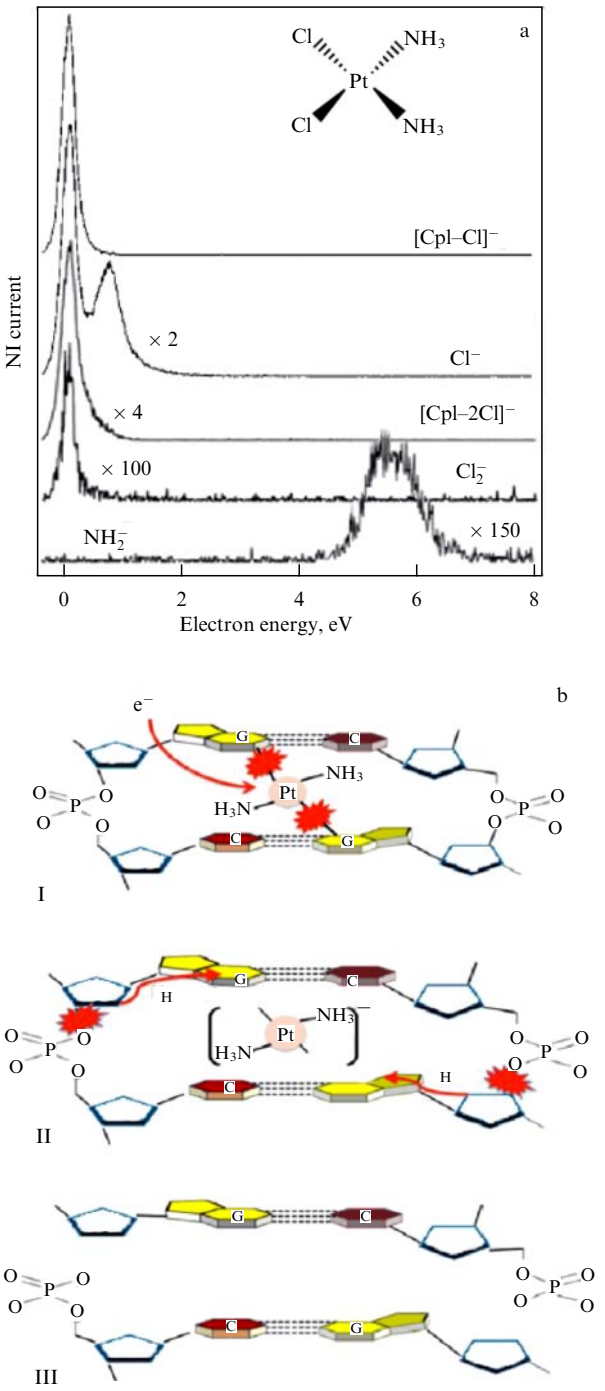

Figure 13. (Color online.) (a) NI currents produced upon DEA by cisplatin (Cpl) molecules as functions of electron energy; (b) proposed mechanism of the sensitizing action of cisplatin caused by the double break of DNA helices: (I) electron attachment by residue of the Cpl molecule in the region of a guanine (G)-cytosine (C) pair, (II) break of Pt–G bonds and attachment of hydrogen atoms by guanine radicals, (III) distortion of the helix structure. (Adapted from [263, 264].)

delivering high radiation doses to tumor regions to destroy cancer cells, minimizing the damage to healthy tissues. It is assumed that platinum drugs, for example, cisplatin, prevent DNA replication due to their ability to enter the structure of this molecule, thereby enhancing the damaging effects of radiation. The radiosensiblity of platinum drugs is due to the activation of molecules after electron attachment with the formation of negative and neutral fragments by the DEA mechanism. It was found that the detachment of two chlorine atoms from a cisplatin molecule [263] occurs similarly to the activation of a given compound with the formation of a $Pt(NH_3)_2^-$ complex responsible for the suppression of DNA replication, as is shown schematically in Fig. 13. The electron acceptor properties of radiosensitizers were studied in numerous papers, for example, [265] (2-fuoroadenin), [266] (chlorine and bromine derivatives of pyrimidines, [267] (hydroxycarbamide), [268] (uracil derivatives), [269] (taurine and thyoprolin), [270] (bromoadenine), [271] (platinum bromide), [272] (nitroimidazoles), and [273] (misonidazole). DEA was studied for amino acids [274, 275], peptides [276–279], nucleosides [280], and model compounds [168, 281]. The main results are generalized in monograph [282] and reviews [283–285].

The possibility of using experimental results obtained in a gas phase to interpret biological processes stimulated by the capture of weakly bound electrons in a cell medium is still being discussed. After reaching a conclusion about the suppression of dissipation with the formation of dehydrogenized fragmented NIs upon microsolvation of uracil and thymine molecules [225], it was shown in [286] that, in the case of halogen-substituted analogs (5-fluoro and 5-bromuracile), MNI decays were observed for the brom-substituted compound at lower electron energies. It was found in [287] that the formation of hydrogen bonds and protonation of nucleotides in an aqueous medium strongly affect the barriers of the DNA break reaction. Hydrated electrons produced during radiotherapeutic action do not damage DNA in fact, whereas the capture of electrons by brom-substituted nucleic bases is a key factor of sensitization [288]. The unified mechanism of DNA damage by low-energy (5–10 eV) electrons is assigned to the appearance of electronically excited resonances [289]. The development of this area will lead to the understanding of fundamental mechanisms of interaction of ionizing radiation with cells of living organisms based on physicochemical methods in accordance with attempts to combine biological studies with methods of molecular and optical physics [290].

4.2 Electron-induced processes in molecules of biologically active compounds

Studies presented in this section are intended to elucidate the role of electronic processes in biological systems at the molecular level within the framework of problems in quantum biology [291, 292]. These new quite deliberative studies [293] based on old ideas [294, 295] attempt to simulate the behavior of xenobiotics (compounds that are foreign to living organisms and contain molecules that often have a high electron affinity) near electron-transport paths in cells. No doubt, quasi-free electrons in a cell medium localized at phase interfaces (lipid–protein–cytosol) are involved in fundamental processes [296, 297], which can be explained quantum-mechanically, as was proposed more than 80 years ago in the pioneering work of Szent-Györgyi [294] and developed by Lovelock [295].

The origin of quasi-free electrons that can be captured by xenobiotic molecules in a cell medium may be related, first, to the respiratory electron transport chain in mitochondria [298, 299] and, second, to ferments of the P450 cytochrome system considered an 'unusual' electron-transport chain [300, 301]. The 'leak' of electrons from the respiratory Complex III (ubiquinol-cytochrome c-oxidoreductase) localized on an internal membrane of mitochondria leads to the formation of a superoxide-anion radical ($^{\bullet}O_2^-$) due to the one-electron reduction of

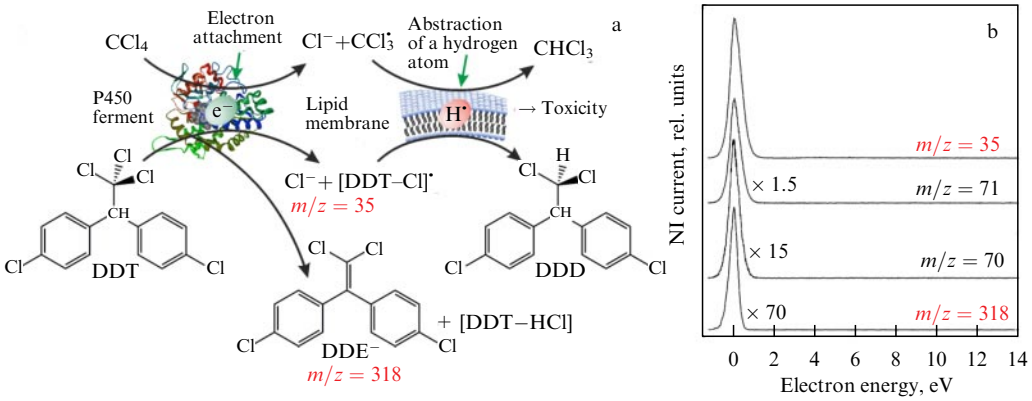

Figure 14. (Color online.) (a) Analogy between the toxicity mechanism postulated for carbon tetrachloride (CCl_4) and assumed for dichlorodiphenyltrichloromethylmethane (DDT): attachment of electrons in the active center of P450 ferment leads to formation of main metabolites — chloroform ($CHCl_3$), dichlorodiphenydichlorethane (DDD), and dichlorodiphenyldichloroethylene (DDE) and active radicals initiating a chain reaction of lipid membrane destruction. (b) DEA spectra for DDT demonstrating formation of dechlorinated radicals and DDE^- in a gas phase during attachment of thermal electrons.

molecular oxygen [298, 299]. It is reasonable to assume that a xenobiotic molecule with an electron affinity higher than for the O_2 molecule ($EA_a = 0.45$ eV [302]) approaching the 'leak' region will compete with O_2 for the capture of electrons [293]. P450 cytochrome ferments localized in an endoplasmic reticulum perform the first phase of metabolism of xenobiotics by successive two-electron reduction [301], which can also result in the formation of an MNI xenobiotic [303].

Papers considered below assume that the formation and destruction of MNIs in a cell medium are governed by resonance mechanisms, and experimental observation in a gas phase can be used as a model for processes of dissociative electron transfer [304, 305]. According to electrochemical studies [303, 306], the MNI dissociation in a condensed medium can occur due to both fast femtosecond 'single-vibration' decays [307, 308] and slow microsecond processes related to the rearrangement of atoms [309, 310], despite the highly possible dissipation of the excess MNI energy in the second case. Note also that reduction reactions in solutions, similar in many respects to the DEA in a gas phase, as shown, for example, for dichlor diphenyl trichlormethylmethane (DDT) [308, 311], are successfully used to simulate the metabolism of xenobiotics by the P450 system [312–314].

The one-electron reduction of the molecule of a model toxic compound, carbon tetrachloride, (CCl_4, $EA_a = 0.8$ eV [315]) by P450 ferments occurs similarly to the gas-phase DEA process [307, 316, 317] and leads to the formation of chloride [318] and a $CCl_3^{\bullet}$ radical. The latter can abstract a hydrogen atom from lipids [319], thereby initiating a chain reaction damaging biological membranes [320] and producing a toxic effect [321]. Simultaneously, the main metabolite of carbon tetrachloride chlorine — a chloroform molecule $CHCl_3$ — is produced. DEA studies of DDT ($EA_a = 1.04$ eV) [311] and some other xenobiotics, including chlorpyrifos [192], peroxybenzoate [322], and brome-containing compounds [323], suggest that a similar toxicity mechanism is possible for many systems containing halogen atoms and other electron-acceptor groups [293], as shown schematically for DDT in Fig. 14. The formation of active radicals is possible when xenobiotic molecules penetrate into mitochondria as well, which is followed by the breaking of membranes and cell destruction [293]. Of special interest are electronic processes in chloroplasts [324], because the 'leak' of electrons from a photosynthetic chain occurs after photoexcitation [325]. This, first, makes possible their capture in high orbitals, thereby opening new MNI decay channels and, second, can be a reason for the difference between biological effects produced by the same compound in respiratory and photosynthetic organisms [326].

Studies of DEA by molecules of polyphenol compounds, for example, flavonoids [327, 328], stilbenes [329], spinchromes [330], and some others [331–334], demonstrate a specific MNI decay caused by the presence of closely spaced hydroxyl groups. Namely, two hydrogen atoms are ejected at the thermal electron energy most efficiently. The ejection is possible only after the break of O–H bonds with the formation of the quinoid structure (C = O double bonds) carrying an additional electron and of a neutral H_2 molecule [327, 331]. The reversibility of similar decays in solutions [335] is especially important in light of the mechanism proposed below. Polyphenol compounds reveal the antioxidant activity related to the neutralization of reactive oxygen species (ROS) [336]. However, the existing mechanism based on the ability to donate a proton [337] cannot completely describe the observed effects.

An alternative mechanism of the protective action of polyphenol compounds near the main source of ROSs involving mitochondrial complex III is illustrated in Fig. 15 for piceatannol ($EA_a = 0.56$ eV [338]). The protective action is caused by three components [338]: (1) the suppression of ROS production due to the capture of 'leaking' electrons [2] from O_2, (2) the production of molecular hydrogen with very strong antioxidant properties [339, 340] near the main source of the oxidative stress, and (3) the formation of a quinoid structure performing electron transport, thereby stimulating cell respiration [341]. Note in conclusion that molecular mechanisms of action of xenobiotics in mitochondria are extremely important for the development of the promising direction in mitochondrial medicine [342, 343], while studies of electron-stimulated reactions in drug molecules can help to find potentially dangerous side effects [344].

[2] Note here that the capture of 'leaking' electrons will be more efficient if the antioxidant molecule has large EA_a. However, as the electron-acceptor properties of a xenobiotic increase, the probability of a toxic effect increases, that limits the values of EA_a for molecules of compounds positively affecting an organism.

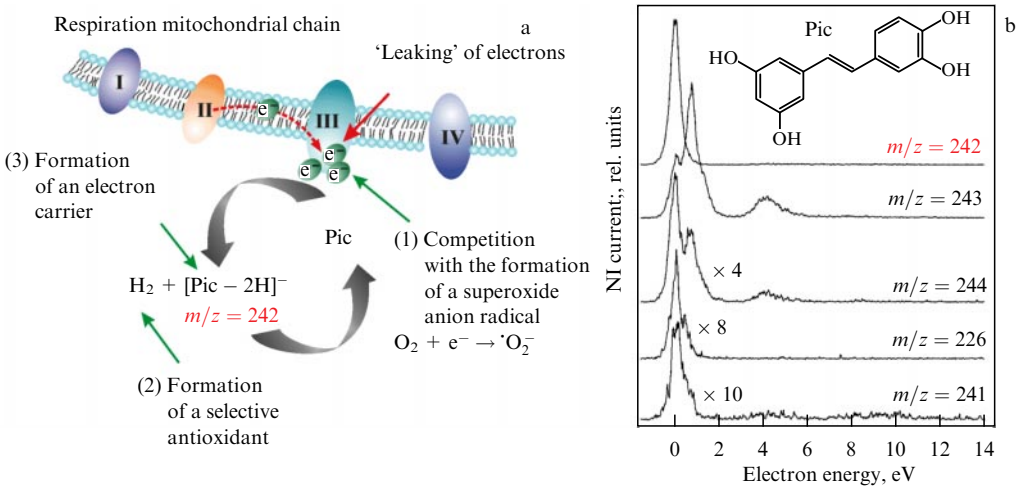

Figure 15. (Color online.) (a) Hypothetical mechanism of reversible [335] protective action of a polyphenol molecule, piceatannol (Pic), near complex III of the electron-transport chain of mitochondria based on trapping 'leaking' electrons, formation of hydrogen and a quinone structure carrying an excess electron; (b) DEA spectra for piceatannol (Pic) demonstrating the efficient detachment of two hydrogen atoms from an MNI at thermal electron energy due to the presence of two hydroxyl groups in the near position.

4.3 Electronic properties and stability of structural elements of organic electronics

One of the main problems preventing wide applications of organic materials in electronics is the absence of their long-term stability [345]. In an environment with an excessive negative charge, in particular, under physiological conditions [346], many organic molecules can be damaged by the DEA mechanism. For example, the capture of electrons by dye molecules used in photogalvanic energy converters leads to the breaking of bonds [120, 347] but depends on the electron resident time near a molecule [120]. Many promising compounds with strong electron-acceptor properties (fullerenes [348], tetracyanoquinoidimethane [349], naphthalene- and perylentetracarbonic dianhydrides [350, 351], condensed aromatic compounds [352–354]) exhibit high stability after the electron attachment and can hold electrons for times from hundreds of microseconds to milliseconds. In this case, fundamental results obtained by DEA spectroscopy about the electron capture and confinement mechanisms and the MNI dynamics [241, 349] are interesting for the development of organic electronics and photonics [355].

Excitation of internal rotations during electron capture can be considered to be the model of an electron-driven molecular rotor [356, 357], which is an actual problem [358]. It was found in [359] that electron capture by an anthracene molecule containing two aniline residues leads to the excitation of the rotational motion and then, depending on the resonance state energy, to the irreversible stop of a motor due to fixation of a 'rotor' or a 'stator' according to the DEA mechanism or to electron autodetachment, which preserves the integrity of the molecular structure, as shown schematically in Fig. 16. Similar effects

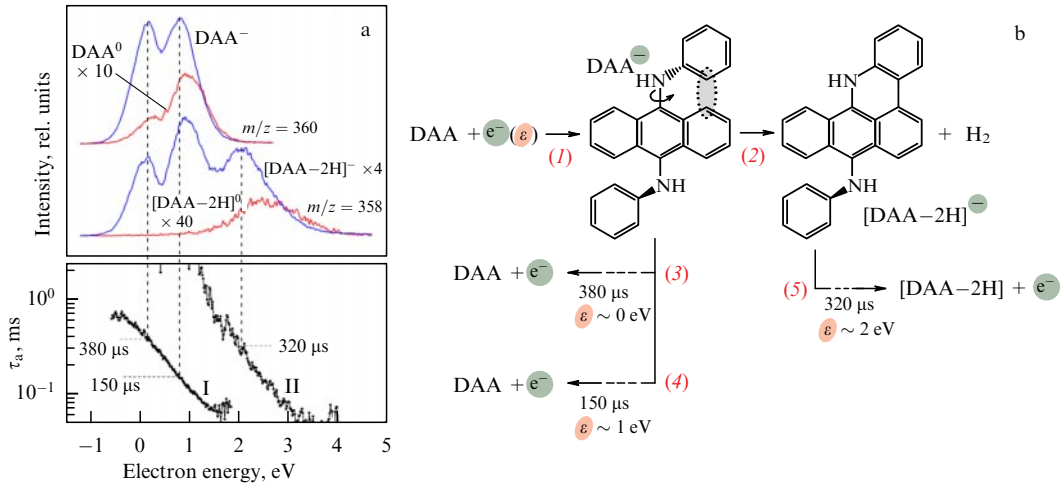

Figure 16. (Color online.) (a) MNI currents for DAA^- and $[DAA-2H]^-$ fragment (blue curves), corresponding signals of neutral components (red curves) and values of $\langle\tau_a\rangle$ for DAA^- (curve I) and $[DAA-2H]^-$ (curve II) in DEA spectra of dianilinedoanthracene (DAA); (b) diagram of formation and main MNI decays: (*1*) electron attachment (three resonances at energies 0, 1, and 2 eV) initiates internal rotation; (*2*) coming together of hydrogen atoms (grey region) leads to detachment of H_2 molecule and formation of a bond in $[DAA-2H]^-$; (*3*, *4*) part of DAA^- forms at energies of ~ 0 and 1 eV, rotates for hundreds of microseconds, and ejects an electron; another part decays in channel (*2*); (*5*) $[DAA-2H]^-$ formed at 2 eV ejects an electron for hundreds of microseconds.

are also observed for other objects [216, 360], and results obtained for isolated molecules are used to describe complex systems in which rotating parts are connected with a massive environment [361, 362]. Note also that the structure of vacant orbitals of isolated π-conjugated molecules in fact completely determines the density of vacant electronic states in the conduction band of ultrathin (10–15 nm) films of similar materials [350, 351] (results obtained by total current spectroscopy [363] and DEA spectroscopy).

Structural transformations of isolated molecules caused by electron capture and the corresponding changes in their electronic structure are another example of results required for describing electron-induced processes in macroscopic objects. Conjugated organic materials with different forbidden bandwidths are of great interest for molecular electronics, in particular, for the development of photogalvanic converters [364, 365]. Polymer films prepared from phthalide monomers belong to a class of broadband polymers and under some conditions have metal-type electric conductivity [366]. Unlike usual π-conjugated systems [367], substituted polyarylenephthalides [368] probably reveal conducting properties in the broken configuration of a phthalide fragment [369]. Recent studies have confirmed the unique behavior of the MNI phthalide in a gas phase — the intramolecular break of a covalent bond [370] — and also predicted similar effects for structurally close molecules [371, 372], which is necessary for understanding the properties of polymer conducting structures [366].

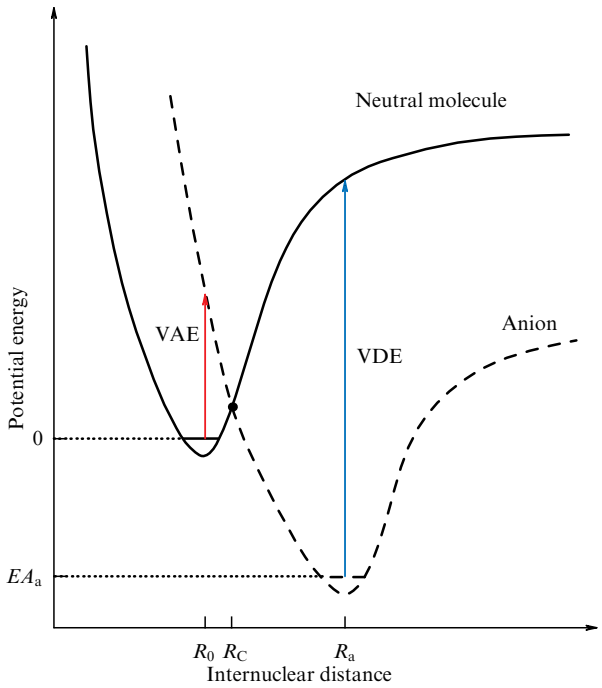

Figure 17. (Color online.) Schemes of molecular (solid curve) and MNI (dashed curve) terms: VAE is vertical attachment energy, VDE is vertical electron detachment energy, EA_a is adiabatic electron affinity, R_0 and R_a are equilibrium internuclear distances in a molecule and anion, respectively, R_C is the term crossing point.

4.4 Estimate of the electron affinity from lifetimes of molecular negative ions

The relation between the electron affinity of a target molecule with the measured electron autodetachment time has not been found to date. As shown in this section, the solution to this problem allows one to propose a new method for estimating the electron affinity of molecules using DEA spectroscopy. Studies of MNI lifetimes attracted the greatest interest in the 1970s [373]. However, with the advent of quadrupole mass analyzers, such work became the prerogative of Russian scientists. The absence of new experimental data resulted in the disappearance of theoretical papers, and interest in these studies arose again only in the 2010s. The formation of MNIs by the VFR mechanism [14, 15, 19] is inherent only in polyatomic systems having positive electron affinity. Because the equilibrium geometries of an ion and a molecule are, generally speaking, different, the ion begins to move in the direction of the total energy minimum, which makes electron ejection impossible until the system returns to the initial geometry. For a diatomic molecule, the value of τ_a is determined by the time nuclei move along the negative term from the distance R_0 (Fig. 17) at which the electron capture occurs to the distance R_C. For $R > R_C$, this state becomes stable.

In the case of a diatomic molecule, a MNI decays during one or several oscillations of nuclei (for the electronic term of the NI in the form of a well), depending on the autodecay term width. Therefore, τ_a for the autodecay term is $10^{-14}-10^{-12}$ s [5]. For polyatomic MNIs, where the energy excess is redistributed between oscillations, the values of τ_a can reach a few ten or even thousands of microseconds at the typical oscillation period of atoms in an ion of 10^{-13}–10^{-11} s [5, 19]. The value of τ_a can be roughly estimated from the expression [5]

$$\tau_a \propto N! \exp(EA_a), \tag{9}$$

where N is the number of active degrees of freedom involved in the MNI geometry transformation. Because $N = 3n - 6$, where n is the number of atoms in a nonlinear molecule, the value of τ_a can be considerable. Because a VFR is related to violation of the Born–Oppenheimer principle and therefore requires a long lifetime of an electron in the scattering potential region, the maximum electron energy is rather low and, as a rule, does not exceed the thermal energy. Otherwise, the electron will bypass the molecule in a time insufficient for nuclei to begin the motion. This fact motivates a search for intermediate electron capture mechanisms providing electron confinement (see Section 3.1). In [373], the expression

$$\tau_a^{-1} = \frac{\Gamma(N)\Pi_{i=1}^{N} h\nu_i'}{\left[\varepsilon + EA_a + \varepsilon_z'(1-\beta w')\right]^{N-1}} \frac{m}{\pi^2\hbar^3} \times \int_0^{\varepsilon_z} \frac{\left[\varepsilon - \varepsilon_f + \varepsilon_z(1-\beta w'')\right]^{N-1}}{\Gamma(N)\Pi_{i=1}^{N} h\nu_i} \varepsilon_f \sigma^{(*)}(\varepsilon_f)\, \mathrm{d}\varepsilon_f \tag{10}$$

is obtained, where m is the electron mass, $1-\beta w'$ is the correction to the internal energy amount, β is a function taking into account the frequency dispersion, ε_z and ε_z' are vibrational energies of the molecule and anion, respectively, and ν_i are vibrational frequencies of the molecule. In this model, the fraction of active degrees of freedom determining the internal energy supply is specified by a choice of fitting parameters w' and w''. This disadvantage is absent in the quantum statistical approach used in [374] to analyze MNIs of fullerene C_{60}. However, model [373] can be simplified without loss of its predictive strength, as was done in [243, 375]. Although the simplified model (see Fig. 17) rigorously describes only a diatomic molecule, it can be used to analyze polyatomic molecules [5, 19], as in the description of decays

of $ClCF_3^-$ [376] and $ClCH_3^-$ [377] by considering the C–Cl bond as the reaction coordinate and 'freezing' the rest of the degrees of freedom. Such a semi-classical dynamic approach provides simulation of fast decays proceeding at the time scale of $\sim 10^{-13}$ s of one oscillation of the halogen–carbon bond.

According to review [378], the equilibrium in a vibrational subsystem of a molecule or an MNI is described as their 'temperature' [374, 378–382]. This approach for molecules became standard long ago; however, for MNIs, the question is whether the complete redistribution of the vibrational energy over internal degrees of freedom has time to occur before the decay. In the case of long-lived MNIs or metastable decays, the energy equidistribution is obviously established, but rapid processes require careful consideration. It was shown recently theoretically [383] and experimentally [378, 379] that the intramolecular energy transfer time for vibrational excitation can be rather small. For example, the energy transfer from the selectively excited vibrational degree of freedom of C–H in a benzene molecule and some other polyatomic molecules can completely occur for times shorter than 50 fs [384]. The experimental study of the dynamics of the intramolecular redistribution of the vibrational energy of the initially excited acetylene-type C–H bond to other modes of the $H-C\equiv C-Si(CH_3)_3$ molecule [385] gives a deexcitation time of 128 ps.

It is reasonable to assume that anions have close vibrational relaxation times and can be described statistically. A molecular negative ion produced near a point R_C (see Fig. 17) moves to the term minimum and, in the case of a diatomic molecule, will return to the initial point in which the autodetachment is an open channel. However, the MNI of a polyatomic molecule moving to the minimum can transfer part of the vibrational energy to other internal degrees of freedom, making the return to the point R_C impossible [378]. As a result, the MNI will oscillate near the equilibrium state value of R_a until a sufficient supply of vibrational energy concentrates on the reaction coordinate for returning to the vicinity of the point R_C. The total vibrational energy stored in the MNI is

$$E_{vib}^- = EA_a + E_{vib}^0 + \varepsilon\,, \tag{11}$$

where E_{vib}^0 is the vibrational energy of the initial molecule and ε is the captured electron energy. In the classical approximation,

$$E_{vib}^0 = Nk_BT\,, \qquad E_{vib}^- = Nk_BT^-\,, \tag{12}$$

where N is the number of internal degrees of freedom, T and T^- are 'temperatures' of the molecule and MNI, respectively. Then, in the Arrhenius approximation, the time to return from the minimum of the MNI term to the point R_C can be described by the expression

$$\tau_a \approx t_0 \exp\left(\frac{EA_a}{k_BT^-}\right) = t_0 \exp\left(\frac{NEA_a}{EA_a + Nk_BT + \varepsilon}\right), \tag{13}$$

where t_0 is the period of anion vibrations in a potential wall, as was shown in [234, 364].

Another physical interpretation of the parameter t_0 is the characteristic time of the distribution of vibrational energy between internal degrees of freedom of the MNI, which can vary from 100 [243] to 500 fs [375], depending on the compound type. Unfortunately, no experimental or theoretical approaches for measuring this quantity exist, but clearly it cannot be smaller than the minimal period of nuclear oscillations in an MNI and probably should not exceed the maximum oscillation period, i.e., it lies in the range from a hundred to a few thousand femtoseconds. With the exception of t_0, expression (13) contains quantities measured in experiments and gives the estimate of EA_a in the form [218, 219, 372, 386]

$$EA_a = \frac{\ln(\tau_a/t_0)(Nk_BT + \varepsilon)}{N - \ln(\tau_a/t_0)}\,. \tag{14}$$

The optimal method for estimating the electron affinity is the study of related compounds, with one of them having the known EA_a [243, 375], which provides an estimate of t_0 [387]. Figure 18 compares the values of EA_a obtained by the electron transfer reaction (ETR) method [4] with calculations by the B3LYP/6-31+G(d) method and calculations using expression (14). The agreement between the ETR and DEA results is quite satisfactory, whereas DFT calculations systematically overstate the value of EA_a by approximately 10% [387–389]. Note that ETR measurements are also based on a comparison with the known value of EA_a, while a more accurate method is the photoelectronic spectroscopy of NIs [390, 391]. Analysis of the EA_a values calculated from (14) showed that the variation in t_0 considerably improves agreement with data in the literature and the value of t_0 does not exceed 1000 fs. Note that the estimate of the amount of vibrational energy from (12) gives overstated values at low temperatures [374] in the denominator of expression (13); however, a similar 'error' also appears in the numerator, because the excess MNI energy is assumed to be evenly distributed over vibrational degrees of freedom. As a result, these inaccuracies are compensated to some degree, leading to acceptable results [218, 219, 243, 372, 375, 386, 387, 392, 393].

Ponomarev and Mazunov noted earlier [394] that 10–30% of the captured electron energy can be spent to change the rotational and translational energy of MNIs, and only about 30% of internal degrees of freedom are involved in the redistribution of the MNI vibrational energy. However, a modification of expressions (13) and (14) taking these facts into account does not lead to good agreement with data in the literature. Khatymov et al. [395] attempted to modify the Arrhenius equation to estimate EA_a for phthalocyanine and tetraphenylporphyrin molecules producing long-lived MNIs for energies above 5 eV using the expression

$$\tau_a = t_0 \exp\left(\frac{NEA_a}{\varepsilon_{vib}^-}\right) \tag{15}$$

instead of (13), where ε_{vib}^-/N corresponds to the mean internal vibrational energy per degree of freedom, and also representing the vibrational energy of the molecule in the quantum approximation [374] as

$$\varepsilon_{vib}^0 = \sum_{j=1}^{N} \frac{\sum_{n=0}^{\infty} g_j\, nh\nu_j \exp(-nh\nu_j/k_BT)}{\sum_{n=0}^{\infty} g_j \exp(-nh\nu_j/k_BT)}\,, \tag{16}$$

where g_j is the degeneracy degree and ν_j is the vibrational frequency. The authors correctly note in [395] that the use in (15) of more realistic values of ε_{vib}^0 calculated by quantum expression (16) instead of classical estimate (12) leads to unacceptable values of $t_0 \sim 10^{-24}-10^{-19}$ s. Obviously, this is explained by the fact that not all the MNI vibrations are involved in the redistribution of the excess energy [373, 394].

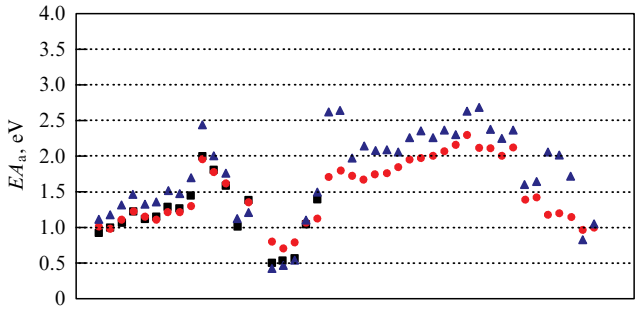

Figure 18. (Color online.) Comparison of EA_a values obtained by ETR (squares) [4] and B3LYP/6-3+G(d) (triangles) methods and from MNI lifetimes (dots) [388]. List of compounds in the order of their arrangement in the plot: 2- and 3-nitrotoluene, 2-, 3-, and 4-fluoronitrobenzene, 2-, 3-, and 4-chloronitrobenzene, 3,4-dichloronitrobenzene, 1,4-dinitrobenzene, 1,4-naphthoquinone, 9,10-anthraquinone, phthalimide, azobenzene, pyrene, benzopyrene, anthracene, tetracene, pentacene, 1,8- and 1,5-dinitroanthraquinone, 1,2-, 1,8-, and 1,4-dihydroxyanthraquinone, 1,2,4-trihydroxyanthraquinon, 2-hydroxy-1,4-, 5-hydroxy-1,4-, 5,8-dihydroxy-1,4-, 3,5-dihydroxy-1,4-, 2,5,8-trihydroxy-1,4-, 2,3,5,7-tetrahydroxy-1,4-, 2,5,6,7-tetrahydroxy-1.4-, 2,5,7,8-tetrahydroxy-3-aceto-1,4-, 2,3,5,7,8-pentahydroxy-1,4-, 2,3,5,7,8-pentahydroxy-3-aceto-1,4 and 2,3,5,6,7,8-sextahydroxy-6-ethyl-1,4-naphthaquinine, 2,5-dichloronithrobenzene, 1,2,3,4,5,6,7-hepta(metoxycarbonyl)-, 1-cyano-2,3,6-trimethoxycarbonyl-4,5 diari-7-trifuoromethyl-, 1,2,3,6-tetramethxycarbonile-4,5-diaryl-7-trifuoromethyl-, 1-metoxy-2,7-dimetyl-3,6-dietoxytoxycarbonyl-4,5-diaryl- and 1,2,4,5,7-pentaaryl-3,5-dietoxitoxicarbonyl-cycloheptatrien.

The decay rate of anions of 5,6,11,12,17,18-hexaazatrinaphthalene and its derivative in the ground electronic state due to autodetachment was estimated from the expression [242]

$$k(\bar{\varepsilon}_{vib}) = \frac{\sigma W^{\pm}(\bar{\varepsilon}_{vib} - \varepsilon_a)}{h\rho(\bar{\varepsilon}_{vib})}, \qquad (17)$$

where ε_a is the activation energy, $W^{\pm}(\bar{\varepsilon}_{vib} - \varepsilon_a)$ is the sum of the states of the activated complex in the interval from zero to $\bar{\varepsilon}_{vib} - \varepsilon_a$ of all degrees of freedom orthogonal to the reaction coordinate, $\rho(\bar{\varepsilon}_{vib})$ is the density of the active states of the anion, and σ is the degeneracy degree of the reaction coordinate. The required parameters were obtained by the DFT method in the PBE/3ζ approximation [396], and the results agree well with experiments and suggest that this approach is promising despite the problem of fitting parameters and cumbersome calculations. Note finally that expression (14) contains the only variable parameter t_0, and gives the estimate of τ_a or EA_a, which is important for describing MNIs with optimal structures significantly different from the geometry of the initial molecule.

4.5 Stabilization mechanisms of long-lived molecular negative ions

The delay of autodetachment during the attachment of thermal electrons by the VFR mechanism [14, 15, 19] (see Section 4.4) is determined by the redistribution dynamics of the excess energy (see Section 3.6). In the epithermal energy region, the SR lifetime is determined by electron tunneling through a centrifugal barrier and is $\sim 10^{-10}-10^{-15}$ s [237], while the EER lifetime cannot exceed the characteristic radiation lifetime of $\sim 10^{-8}$ s. There are several hypotheses explaining the nature of MNI transitions from the initial short-lived state to the long-lived state observed in the epithermal region:

(1) formation of an EER and stabilization of the MNI due to a nonradiative transition to the ground electronic state [397, 398],

(2) formation of SRs and internal MNI conversion in the ground electronic state [193, 238, 239, 399–401],

(3) formation of an EER and transformation of the ion doublet to an ion quartet by intersystem crossing [402],

(4) MNI transitions to more stable conformations [394, 403, 404],

(5) electron attachment with excitation of plasma modes [405].

Hypotheses 1–4 explain the existence of long-lived MNIs in several resonances in the energy range from 0 to ~ 4 eV. Hypothesis 5 explains a broad and in fact continues energy range from 0 to 15 eV in which long-lived MNIs of fullerene and its derivatives are observed [406–408]. The authors of [405] considered in fact resonances of a new type when the incident electron spends its energy to excite plasma oscillations and is captured with an energy close to zero. However, obviously, this mechanism does not guarantee at all the existence of long-lived MNIs, because the lifetime of plasmons is $\sim 10^{-14}-10^{-15}$ s [409]. Note that nothing is known about the behavior of a fullerene MNI after electron capture [410], although the electron autodetachment rate constant is completely determined by the MNI excess energy, meaning that the ground electronic state of fullerene MNIs has a long lifetime.

Analysis of the literature shows that, independently of the mechanism of initial electron attachment, the long lifetime of MNIs in the epithermal energy region is determined not by the initial but by the final long-lived electronic state, which is obviously the ground electronic state produced from a short-lived state due to a series of fast ($10^{-12}-10^{-14}$ s) [411–413] nonradiative transitions without multiplicity changing (internal conversion). In this case, the radiative energy losses are absent and all the excess energy of the MNIs is converted into vibrational energy. This mechanism is confirmed by at least three experimentally established facts:

(1) rapid monotonic decrease in $\langle\tau_a\rangle$ with electron energy [19, 193, 238, 239, 251, 370, 397, 398, 400–402],

(2) decrease in $\langle\tau_a\rangle$ with increasing temperature at a fixed resonance energy [193, 238, 239, 251, 400, 410],

(3) gradual disappearance of the temperature dependence of $\langle\tau_a\rangle$ with increasing resonance energy [238, 239, 251].

These observations can be explained without complicated calculations. Namely, the MNI lifetime for molecules with positive electron affinity is completely determined by the excess energy and decreases with increasing E_{exc}. From the mathematical point of view, $\langle\tau_a\rangle$ is a unique monotonically decreasing function of the excess MNI energy $\langle\tau_a\rangle = f(E_{exc}) = f(EA_a + E_{vib}(T) + \varepsilon)$. In the absence of radiation losses, the value of E_{exc} increases with increasing ε at $T = \text{const}$ and with increasing T at $\varepsilon = \text{const}$. As ε increases for the fixed temperature range $T_1 < T < T_2$, the proportion of mean vibrational energy $E_{vib}(T)/E_{exc}$ decreases.

From the theoretical point of view, the final electronic state of long-lived MNIs obtained due to internal conversion is analogous to the state formed during thermal electron capturing,[3] but for excess energy higher by ε, i.e., $\langle\tau_a\rangle$ is also

[3] Note that such a state is completely similar to the autoionization state of fragmented ions with the vibrational excitation energy exceeding the electron affinity of radicals [19]. Measurement of the lifetimes of such ions was difficult sometimes because of a small signal intensity, but in some cases it was possible [414].

determined by statistical laws. For example, E_{exc} for the anthraquinone MNI can reach ~ 4 eV ('effective' vibrational temperature [400] $T_{ve} \approx 1200$ K), while for MNIs of fullerene and its derivatives, ~ 20 eV [406, 407] ($T_{ve} \approx 1950$ K). To answer the question of whether MNIs with such a high vibrational energy will be long-lived, the temperature dependence of $\langle \tau_a \rangle$ was studied for azobenzene MNIs with a static mass spectrometer using the ISK model (see Section 3.6). The number $W(E)$ of vibrational degrees of freedom of the molecule and ion was determined by direct calculations, which made it possible to express them in terms of the functions of density $\rho_n(E)$ and $\rho_i(E)$ of the corresponding energy state and to use the main formula of the ISK model in the form

$$\tau_a(E_v, \varepsilon) = \tau_0 \frac{\rho_i(EA_a + E_v + \varepsilon)}{\rho_n(E_v + \varepsilon)}, \qquad (18)$$

where E_v is the vibrational energy.

The initial Boltzmann distribution of molecules was calculated from the expression

$$P(E_v, T) = \frac{\rho_n(E_v)\exp(-E_v/k_B T)}{\Pi_{i=1}^{3N-6}\left[1-\exp(-hc\omega_i/k_B T)\right]^{-1}}, \qquad (19)$$

where ω_i is the frequency of the ith molecular vibration and the electron capture cross section $\sigma(\varepsilon)$ was simulated by Gaussians. The values of τ_a and the shape of the azobenzene MNI current calculated at several temperatures reproduced experimental data with an error of $\sim 2-10\%$, which confirms the correctness of the statistical ISK model and the assumption that MNI stabilization during the attachment of epithermal electrons occurs due to internal conversion. Obviously, each MNI has its own critical excess energy at which τ_a becomes smaller than 1 μs. It is convenient to define this energy per vibrational degree of freedom for a correct comparison of different MNIs. For example, these energies for MNIs of azobenzene [239], fullerene [406–408], and anthraquinone [238] are ~ 0.05 eV, ~ 0.1 eV, and ~ 0.07 eV, respectively.

Figure 19 shows the energy level diagram (similar to the Jablonski diagram in photochemistry) of competing radiative and nonradiative processes in MNIs produced using the SR mechanism. The diagram is constructed for the lowest-energy SR by ignoring dissociation processes (assuming that they are either unlikely or do not have enough energy to occur) and conformation transitions. One can see from the diagram that the SR evolution is determined by the competition of autodetachment and internal conversion. In this case, it is necessary to distinguish two types of autodetachment processes: from the MNI initial state (femtosecond processes 2 and 3) and from MNIs relaxed due to internal conversion to the ground electronic state (microsecond processes 5 and 6). Experimental data on the rate constants of internal conversion of MNIs are absent, but we can assume that they are close to these rates for molecules, i.e., $10^{12}-10^{14}$ s^{-1} [411–413]. In the case in Fig. 19, the main competing processes are reactions 2–4.

In the alternative concept of MNI stabilization during electron attachment by the EER mechanism with the transformation of an ion doublet to an ion quartet [402], the internal conversion efficiency is assumed to be low due to the large excess energy of the MNI ground electronic state. However, the consideration of internal conversion and a

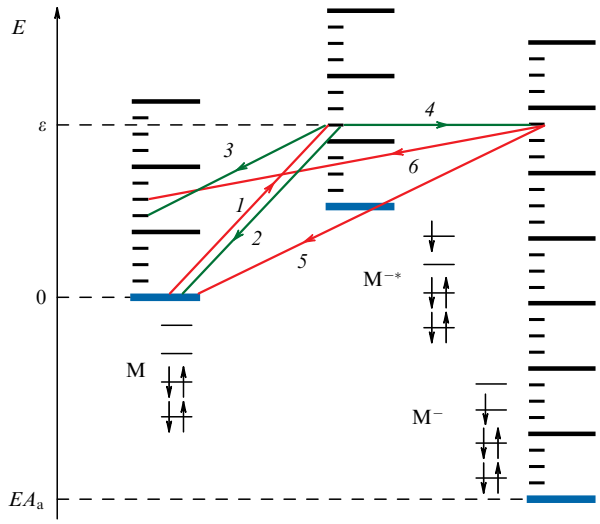

Figure 19. (Color online.) Formation and decay of a shape resonance; main competing processes are shown in green. (*1*) Electron attachment by a target molecule in the ground vibronic state M; (*2*, *3*) electron autodetachment from initial short-lived resonance state M^{-*} to ground and excited vibrational-rotational state M; (*4*) nonradiative transition from M^{-*} to long-lived electronic state M^-; (*5*, *6*) electron autodetachment from M^- to ground and excited vibrational-rotational state M. Ground vibronic state is shown by long blue line, vibrational states in the ground electronic state are shown by long black lines, and rotational levels of the corresponding electronic-vibrational state are shown by short black lines.

similar consideration of the EER evolution lead to the same results as in the SR case (Fig. 20), whereas intersystem crossing, as a spin inversion process, corresponds to less probable relativistic effects. The intersystem crossing rate is usually 2–3 orders of magnitude lower than the internal conversion rate, i.e., the latter is the most probable competing process. Even if we assume that intersystem crossing for molecules studied [402] is more probable, it remains unclear how this concept agrees with temperature effects and the dependence of $\langle \tau_a \rangle$ on ε. It is not by chance that the final state, the M_q^- ion quartet, has a configuration different from that of the initial M^{-*} ion doublet, i.e., intersystem crossing is accompanied by conformational changes, so that M_q^- proves to be in fact devoid of a vibrational energy supply, and only then can its further behavior be explained by electronic effects [402].

In concluding this section, we consider the possibility of using modern theories of nonradiative transitions in polyatomic molecules [411–413] to describe MNIs. Because of the short duration of the exciting pulse and high density of vibronic states, molecules are excited to nonstationary states [412, 415]. In the case of MNIs excited by electron pulses, the electron capture time of $\sim 10^{-15}$ s is estimated by the electron free flight time over a distance equal to the effective diameter of the molecule. The 1-eV electron flies over a distance of 3 Å during $\sim 5 \times 10^{-16}$ s, so the natural width of the exciting pulse is ~ 1.3 eV. The density of vibrational states of azobenzene molecules in the maximum of their distribution at a temperature of 353 K obtained by direct calculations is $\sim 4.6 \times 10^8$ eV^{-1}, i.e., the incident electron has time to 'interact' with $\sim 6 \times 10^8$ vibrational states, while the nonstationary MNI state produced is a mixture of the order of 10^8 stationary states. During mixing of this nonstationary state, the nuclear motion becomes stochastic, as in the VFR case, or

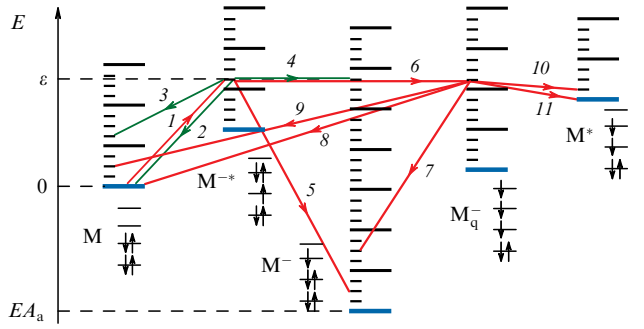

Figure 20. (Color online.) Formation and decay of an electronically excited resonance; main competing processes are shown in green. (*1*) Electron attachment by a target molecule in ground vibronic state M; (*2*, *3*) electron autoattachment from initial short-lived (M^{-*}) or long-lived (M^-) resonance states to ground and excited vibrational-rotational state M; (*4*) nonradiative transition from M^{-*} to long-lived ground electronic state M^- (internal conversion); (*5*) radiative transition from M^{-*} to long-lived ground electronic state M^-; (*6*) nonradiative transition from M^{-*} to ion quartet M_q^- (intersystem crossing); (*7*) spin flip-flop radiative transition (phosphorescence) from M_q^- to M^-; (*8*, *9*) electron autodetachment from M_q^- to ground and excited vibrational-rotational state M; (*10*, *11*) electron autodetachment from M_q^- to ground and excited triplet state M^*.

an irreversible nonradiative transition to a lower electronic state occurs. The probability of this transition increases with increasing density of vibronic states of the lower electronic state at a vibrational energy equal to the nonradiative transition energy. The density of such vibronic states for an MNI is higher than that for a molecule, because the vibrational energy of an MNI is higher by the value of EA_a and is $\sim 3.2 \times 10^{25}$ eV^{-1} for azobenzene, i.e., nonradiative transitions in MNIs are much more probable than in neutral molecules.

5. Conclusions

A comprehensive detailed consideration of the problem indicated in the title is obviously far beyond the scope of our paper, especially taking into account the fact that the last review in this field was published in Russian more than 20 years ago [5]. Nevertheless, based on the material presented here, we can mention some prospects for studying resonance electron scattering. One trend is the complication of objects, including biological structures [284], molecules introduced into clusters [416] and adsorbed on surfaces [417], and structural elements of organic electronics [418]. Traditional experimental methods, including molecular beam preparation, allow the study of these objects; however, the theoretical description of electron-induced processes in large molecules encounters considerable difficulties [29–31]. Therefore, it is necessary to develop methods for describing the DEA by polyatomic molecules for interpretation of experimental results and describe evolution processes from the moment of rapid 'vertical' electron attachment to the microsecond and millisecond MNI decay, which at present is impossible even using imitation simulations [200].

One of the most important problems, which was partly solved for neutral molecules [419–422], is related to the paths and the rate of motion of excess energy over the vibrational degrees of freedom of MNIs, which takes into account the energy exchange between normal vibrations due to their interaction and is described in anharmonic approximations [423]. The development of this area will make a substantial contribution to the description of mechanisms of metastable decays and various MNI dissipation channels. At present, these effects are only mentioned based on DEA observations of structurally close molecules at the microsecond time scale [120], while the energy redistribution in MNIs determining key autodetachment and dissociation processes does not have a theoretical description, even in the case of SF_6^- [147, 424]. Note here also the opposite case of existing highly excited localized vibrational states of polyatomic neutral molecules [425, 426]. A focused search for the manifestation of local modes using the DEA spectroscopy method will help to open new MNI stabilization mechanisms.

To understand the electron capture process at the initial moment, it is very important to know fundamental mechanisms and temporal characteristics of competing femtosecond processes, which lead either to rapid electron detachment or to a series of nonradiative transitions delaying autodetachment and making dissociative decays possible. An accurate description of these phenomena requires solving complex quantum-mechanical problems, but it will give a detailed picture of the initial moment of electron attachment followed by the motion of the excess energy in MNIs. In particular, it is necessary to have *ab initio* estimates of SR lifetimes [427, 428] and rate constants of internal conversion for MNIs, which at present are known only for neutral molecules [411–413].

Concerning new experimental methods, quite promising is the recently developed velocity slice imaging technique [429]. However, the method of electron transmission spectroscopy [7, 8, 121], which is quite rare at present, has not lost its significance at all, especially as a source of information about fast resonance processes supplementing the results of DEA spectroscopy at the microsecond time scale [254]. To develop applied and interdisciplinary directions, it is necessary to estimate absolute DEA cross sections [430] for measuring quantitative characteristics of elementary processes. Promising studies of large objects are closely related to the development of techniques for obtaining molecular beams, including experiments with clusters. Note also the possibility of changing the time scale of mass-spectrometric experiments, which provides additional information on the MNI evolution [254].

The combined efforts of numerous scientific groups in studies of radiosensitizers will probably give the most important results for DEA applications in radiation biology [431]. This area is quite closely related to the use of nanoparticles in medicine [432–434] involving reactions of dissipative electron transfer [435, 436]. In addition, two broad areas in applications of results in molecular electronics and biochemistry have been initiated, in particular, in actual fields of mitochondrial medicine, precise drug delivery, determination of the molecular mechanisms of action and side effects of drugs, mechanisms of toxicity and action of antioxidants, and studies of the electronic properties of natural compounds [293]. In addition, the results discussed above can find important applications in agriculture related to the study of action mechanisms of herbicides and inductors of plant stability to environmental stresses [324], and also in the effects of xenobiotics in photosensitizing organisms [326].

Note in conclusion that resonance scattering and DEA studies have not lost at all their fundamental importance, relevance, and outlook, especially taking into account the goal of achieving an understanding of many processes in a variety of fields of knowledge at the level of individual

molecules and their elementary interactions. In domestic science, contrary to common sense, the situation seems to be determined again by historically political factors, which at present is leading this field of study to complete disappearance. However, undoubtedly, resonance scattering and DEA studies in the work of foreign colleagues will be rapidly developed in the nearest future according to the requirements of modern science.

Acknowledgments. The authors thank the reviewer for their useful remarks. The study was supported by the Russian Foundation for Basic Research (project no. 19-12-50238).

References

1. Thomson J J *Phil. Mag.* **21** 225 (1911)
2. Thomson J J *Phil. Mag.* **41** 510 (1921)
3. Lacmann K *Adv. Chem. Phys.* **42** 513 (1980)
4. Kebarle P, Chowdhury S *Chem. Rev.* **87** 513 (1987)
5. Illenberger E, Smirnov B M *Phys. Usp.* **41** 651 (1998); *Usp. Fiz. Nauk* **168** 731 (1998)
6. Massey H S W *Rev. Mod. Phys.* **28** 199 (1956); Translated into Russian: *Usp. Fiz. Nauk* **64** 589 (1958)
7. Jordan K D, Burrow P D *Chem. Rev.* **87** 557 (1987)
8. Jordan K D, Burrow P D *Acc. Chem. Res.* **11** 341 (1978)
9. Khvostenko V I, Dukel'skii V M *Sov. Phys. JETP* **6** 657 (1958); *Zh. Eksp. Teor. Fiz.* **33** 851 (1957)
10. Schulz G J *Rev. Mod. Phys.* **45** 378 (1973)
11. Schulz G J *Rev. Mod. Phys.* **45** 423 (1973)
12. O'Malley T F *Phys. Rev.* **150** 14 (1966)
13. Taylor J R *Scattering Theory. The Quantum Theory on Nonrelativistic Collisions* (New York: Wiley, 1972); Translated into Russian: *Teoriya Rasseyaniya: Kvantovaya Teoriya Nerelyativistskikh Stolknovenii* (Moscow: Mir, 1975)
14. Christophorou L G (Ed.) *Electron-Molecule Interactions and Their Applications* (New York: Academic Press, 1984)
15. Illenberger E, Momigny J *Gaseous Molecular Ions. An Introduction to Elementary Processes Induced by Ionization* (Darmstadt: Steinkopff Verlag, 1992)
16. Čársky R, Čurík P (Eds) *Low-Energy Electron Scattering from Molecules, Biomolecules and Surfaces* (Boca Raton, FL: CRC Press. Taylor and Francis Group, 2012)
17. Shimamura I, Takayanagi K (Eds) *Electron-Molecule Collisions* (New York: Plenum Press, 1984)
18. Huo W M, Gianturco F A (Eds) *Computational Methods for Electron-Molecule Collisions* (New York: Plenum Press, 1995)
19. Khvostenko V I *Mass-spektrometriya Otritsatel'nykh Ionov v Organicheskoi Khimii* (Mass Spectrometry of Negative Ions in Organic Chemistry) (Moscow: Nauka, 1981)
20. Khvostenko V I, Tolstikov G A *Russ. Chem. Rev.* **45** 127 (1976); *Usp. Khim.* **45** 251 (1976)
21. Allan M *J. Electron Spectrosc. Relat. Phenom.* **48** 219 (1989)
22. Stamatovic A, Schulz G J *Rev. Sci. Instrum.* **39** 1752 (1968)
23. Stamatovic A, Schulz G J *Rev. Sci. Instrum.* **41** 423 (1970)
24. Chutjian A, Garscadden A, Wadehra J M *Phys. Rep.* **264** 393 (1996)
25. Hotop H et al. *Adv. Atom. Mol. Opt. Phys.* **49** 85 (2003)
26. Hotop H, Ruf M-W, Fabrikant I I *Phys. Scripta* **2004** (T110) 22 (2004)
27. Fabrikant I I *J. Phys. Conf. Ser.* **204** 012004 (2010)
28. Andersen T *Phys. Rep.* **394** 157 (2004)
29. Fabrikant I I et al. *Adv. Atom. Mol. Opt. Phys.* **66** 545 (2017)
30. Krishnakumar E, Prabhudesai V S, in *Quantum Collisions and Confinement of Atomic and Molecular Species, and Photons. Select Proc. of the 7th Topical Conf. of ISAMP 2018* (Springer Proc. in Physics, Vol. 230, Eds P C Deshmukh et al.) (Singapore: Springer, 2019) p. 20
31. Ingólfsson O *Low-Energy Electrons: Fundamentals and Applications* (Boca Raton, FL: CRC Press, 2019)
32. Burrow P D, Modelli A *SAR QSAR Environ. Res.* **24** 647 (2013)
33. Ortiz J V *WIREs Comput. Mol. Sci.* **3** 123 (2013)
34. Spence D, Schulz G J *J. Chem. Phys.* **58** 1800 (1973)
35. Acharya P K, Kendall R A, Simons J *J. Am. Chem. Soc.* **106** 3402 (1984)
36. Gerchikov L G, Gribakin G F *Phys. Rev.* **A 77** 042724 (2008)
37. Christophorou L G et al. *J. Phys. D* **14** 1889 (1981)
38. Lu Q-B, Sanche L *Phys. Rev. Lett.* **87** 078501 (2001)
39. Schmidt F, Swiderek P, Bredehöft J H *ACS Earth Space Chem.* **3** 1974 (2019)
40. Boyer M C et al. *Surf. Sci.* **652** 26 (2016)
41. Christophorou L G, Olthoff J K *Fundamental Electron Interactions with Plasma Processing Gases* (Berlin: Springer, 2012)
42. Arumainayagam C R et al. *Surf. Sci. Rep.* **65** 1 (2010)
43. Luo J et al. *Chemosphere* **131** 17 (2015)
44. Pimblott S M, LaVerne J A *Radiat. Phys. Chem.* **76** 1244 (2007)
45. Böhler E, Warneke J, Swiderek P *Chem. Soc. Rev.* **42** 9219 (2013)
46. Huels M A et al. *Int. J. Mass Spectrom.* **277** 256 (2008)
47. Byakov V M, Stepanov S V *Phys. Usp.* **49** 469 (2006); *Usp. Fiz. Nauk* **176** 487 (2006)
48. Klenov G I, Khoroshkov V S *Phys. Usp.* **59** 807 (2016); *Usp. Fiz. Nauk* **186** 891 (2016)
49. Boudaïffa B et al. *Science* **287** 1658 (2000)
50. Khatymova L Z, Mazunov V A, Khatymov R V *Istoriya Nauki Tekh.* (3) 11 (2011)
51. Kazanskii A K, Fabrikant I I *Sov. Phys. Usp.* **27** 607 (1984); *Usp. Fiz. Nauk* **143** 601 (1984)
52. Eletskii A V, Smirnov B M *Sov. Phys. Usp.* **28** 956 (1985); *Usp. Fiz. Nauk* **147** 459 (1985)
53. Vostrikov A A, Samoilov I V *Pis'ma Zh. Eksp. Teor. Fiz.* **18** (7) 58 (1992)
54. El'kin Yu N et al. *Zh. Analit. Khim.* **42** 2232 (1987)
55. Lend'el V I, Navrotskii V T, Sabad E P *Sov. Phys. Usp.* **30** 220 (1987); *Usp Fiz. Nauk* **151** 425 (1987)
56. Zapesochnyi I P et al. *Sov. Phys. Dokl.* **19** 77 (1974); *Dokl. Akad. Nauk SSSR* **214** 1288 (1974)
57. Sidorov L N, Korobov M V, Zhuravleva L V *Mass-spektral'nye Termodinamicheskie Issledovaniya* (Mass-Spectral Thermodynamic Studies) (Moscow: Izd. MGU, 1985)
58. Drukarev G F *Collisions of Electrons with Atoms and Molecules* (New York: Plenum Press, 1987); Translated from Russian: *Stolknoveniya Elekronov s Atomami i Molekulami* (Moscow: Nauka, 1978)
59. Fabrikant I I *Sov. Phys. JETP* **46** 693 (1977); *Zh. Eksp. Teor. Fiz.* **73** 1317 (1977)
60. Kukhta A V et al. *Chem. Phys. Lett.* **373** 492 (2003)
61. Kukhto A V *J. Appl. Spectrosc.* **65** 722 (1998)
62. Schippers S et al. *J. Phys. B* **52** 171002 (2019)
63. Mason N J *J. Phys. Conf. Ser.* **565** 012001 (2014)
64. Christophorou L G *Chem. Rev.* **76** 409 (1976)
65. Smirnov B M *Phys. Usp.* **45** 1251 (2002); *Usp. Fiz. Nauk* **172** 1411 (2002)
66. Smith D, Ŝpanêl P *Adv. Atom. Mol. Opt. Phys.* **32** 307 (1994)
67. de Urquijo J et al. *Eur. Phys. J. D* **55** 637 (2009)
68. de Urquijo J et al. *Eur. Phys. J. D* **51** 241 (2009)
69. Yousfi M et al. *IEEE Trans. Plasma Sci.* **37** 764 (2009)
70. White R D et al. *Eur. Phys. J. D* **68** 125 (2014)
71. Casey M J et al. *J. Chem. Phys.* **147** 195103 (2017)
72. Kopyra J et al. *Acta Phys. Slovaca* **55** 447 (2005)
73. Nikitović Ž D et al. *Plasma Sources Sci. Technol.* **18** 035008 (2009)
74. Dujko S et al. *Jpn. J. Appl. Phys.* **50** 08JC01 (2011)
75. Dahl D A, Teich T H, Franck C M *J. Phys. D* **45** 485201 (2012)
76. Haefliger P, Hösl A, Franck C M *J. Phys. D* **51** 355201 (2018)
77. Wnorowski K et al. *Chem. Phys. Lett.* **634** 203 (2015)
78. Wnorowski K et al. *Chem. Phys. Lett.* **667** 272 (2017)
79. Michalczuk B, Barszczewska W *Chem. Phys. Lett.* **740** 137056 (2020)
80. Tabrizchi M, Abedi A *J. Phys. Chem. A* **108** 6319 (2004)
81. Feng H et al. *Int. J. Mass Spectrom.* **305** 30 (2011)
82. Han H et al. *Chinese J. Chem. Phys.* **24** 218 (2011)
83. Kučera M et al. *Eur. Phys. J. D* **67** 234 (2013)
84. Krishnakumar E et al. *Phys. Rev. A* **56** 1945 (1997)
85. Rangwala S A, Kumar S V K, Krishnakumar E *Phys. Rev. A* **64** 012707 (2001)
86. Rangwala S A, Krishnakumar E, Kumar S V K *Phys. Rev. A* **68** 052710 (2003)

87. Fedor J, May O, Allan M *Phys. Rev. A* **78** 032701 (2008)
88. May O, Fedor J, Allan M *Phys. Rev. A* **80** 012706 (2009)
89. May O, Kubala D, Allan M *Phys. Rev. A* **82** 010701 (2010)
90. Janečková R et al. *Phys. Rev. Lett.* **111** 213201 (2013)
91. Chandler D W, Houston P L *J. Chem. Phys.* **87** 1445 (1987)
92. Eppink A T, Parker D H *Rev. Sci. Instrum.* **68** 3477 (1997)
93. Townsend D, Minitti M P, Suits A G *Rev. Sci. Instrum.* **74** 2530 (2003)
94. Nandi D et al. *Rev. Sci. Instrum.* **76** 053107 (2005)
95. Prabhudesai V S, Nandi D, Krishnakumar E *J. Phys. B* **39** L277 (2006)
96. Jagutzki O et al. *Nucl. Instrum. Meth. Phys. Res. A* **477** 244 (2002)
97. Adaniya H et al. *Rev. Sci. Instrum.* **83** 023106 (2012)
98. Nag P, Nandi D *Phys. Rev. A* **91** 052705 (2015)
99. Krishnakumar E et al. *Phys. Rev. Lett.* **106** 243201 (2011)
100. Szymańska E et al. *Phys. Chem. Chem. Phys.* **15** 998 (2013)
101. Rescigno T N et al. *Phys. Rev. A* **93** 052704 (2016)
102. Moradmand A et al. *Rev. Sci. Instrum.* **84** 033104 (2013)
103. Wu B et al. *Rev. Sci. Instrum.* **83** 013108 (2012)
104. Wu B et al. *Phys. Rev. A* **85** 052709 (2012)
105. Tian S X et al. *Phys. Rev. A* **88** 012708 (2013)
106. Dreiling J M, Gay T J *Phys. Rev. Lett.* **113** 118103 (2014)
107. Dreiling J M et al. *Phys. Rev. Lett.* **116** 093201 (2016)
108. Rosenberg R A, in *Electronic and Magnetic Properties of Chiral Molecules and Supramolecular Architectures* (Topics in Current Chemistry, Vol. 298, Eds R Naaman, D N H Beratan, D N Waldeck) (Berlin: Springer-Verlag, 2011) p. 279
109. Davankov V A *Zh. Fiz. Khim.* **83** 1405 (2009)
110. Dreiling J M, Burtwistle S J, Gay T *J. Appl. Opt.* **54** 763 (2015)
111. Li Z et al. *Phys. Rev. Lett.* **119** 053402 (2017)
112. Edelson D, Griffiths J E, McAfee K B (Jr.) *J. Chem. Phys.* **37** 917 (1962)
113. Ibănescu B C et al. *Phys. Chem. Chem. Phys.* **9** 3163 (2007)
114. Abdoul-Carime H et al. *Eur. Phys. J. D* **35** 399 (2005)
115. Ptasińska S et al. *J. Chem. Phys.* **120** 8505 (2004)
116. Meißner R et al. *J. Mass Spectrom.* **54** 802 (2019)
117. Bjarnason E H et al. *Eur. Phys. J. D* **68** 121 (2014)
118. Papp P et al. *J. Chem. Phys.* **125** 204301 (2006)
119. Modelli A, Jones D, Pshenichnyuk S A *J. Phys. Chem. C* **114** 1725 (2010)
120. Pshenichnyuk S A, Modelli A *Int. J. Mass Spectrom.* **294** 93 (2010)
121. Modelli A et al. *Chem. Phys. Lett.* **163** 269 (1989)
122. Zawadzki M, Luxford T F M, Kočišek *J. Phys. Chem. A* **124** 9427 (2020)
123. Matejčík, Š et al. *Int. J. Mass Spectrom.* **223–224** 9 (2003)
124. Lehr L, Miller W H *Chem. Phys. Lett.* **250** 515 (1996)
125. Christophorou L G, Datskos P G *Int. J. Mass Spectrom. Ion Process.* **149–150** 59 (1995)
126. Srivastava S K, Orient O J *Phys. Rev. A* **27** 1209 (1983)
127. Chen C L, Chantry P J *J. Chem. Phys.* **71** 3897 (1979)
128. Christophorou L G et al. *Phys. Rev. Lett.* **58** 1316 (1987)
129. Makarov G N *Phys. Usp.* **58** 670 (2015); *Usp. Fiz. Nauk* **185** 717 (2015)
130. Christophorou L G, Olthoff J K *Adv. Atom. Mol. Opt. Phys.* **44** 155 (2001)
131. Desfrançois C, Abdoul-Carime H, Schermann J-P *Int. J. Mod. Phys. B* **10** 1339 (1996)
132. Gutowski M et al. *Int. J. Quantum Chem.* **64** 183 (1997)
133. Rogers J P, Anstöter C S, Verlet J R R *Nat. Chem.* **10** 341 (2018)
134. Kunin A, Neumark D M *Phys. Chem. Chem. Phys.* **21** 7239 (2019)
135. Scheer A M et al. *Phys. Rev. Lett.* **92** 068102 (2004)
136. Sommerfeld T *J. Phys. Conf. Ser.* **4** 245 (2005)
137. Jordan K D, Wang F *Annu. Rev. Phys. Chem.* **54** 367 (2003)
138. Simons J *J. Phys. Chem. A* **112** 6401 (2008)
139. Bull J N, Verlet J R R *Sci. Adv.* **3** e1603106 (2017)
140. Güthe F et al. *Astrophys. J.* **555** 466 (2001)
141. Li Z et al. *Phys. Rev. Lett.* **122** 073002 (2019)
142. Sommerfeld T, Davis M C *J. Chem. Phys.* **152** 054102 (2020)
143. Castellani M E, Anstöter C S, Verlet J R R *Phys. Chem. Chem. Phys.* **21** 24286 (2019)
144. Anusiewicz I, Skurski P, Simons J *J. Phys. Chem. A* **124** 2064 (2020)
145. Zhu G-Z, Liu Y, Wang L-S *Phys. Rev. Lett.* **119** 023002 (2017)
146. Liu G et al. *Phys. Chem. Chem. Phys.* **21** 18310 (2019)
147. Fabrikant I I *J. Phys. B* **49** 222005 (2016)
148. Fabrikant I I et al. *J. Chem. Phys.* **136** 184301 (2012)
149. Fabrikant I I *Eur. Phys. J. D* **72** 96 (2018)
150. Sanche L et al. *Phys. Rev. Lett.* **75** 3568 (1995)
151. Nagesha K, Sanche L *Phys. Rev. Lett.* **78** 4725 (1997)
152. Bass A D et al. *J. Phys. Chem.* **99** 6123 (1995)
153. Ayotte P et al. *J. Chem. Phys.* **106** 749 (1997)
154. Turner J E *Am. J. Phys.* **45** 758 (1977)
155. Garrett W R *Mol. Phys.* **24** 465 (1972)
156. Fabrikant I I *Phys. Rev. A* **43** 3478 (1991)
157. Burke P G, Tennyson J *Mol. Phys.* **103** 2537 (2005)
158. Fabrikant I I *J. Phys. B* **10** 1761 (1977)
159. Lane A M, Thomas R G *Rev. Mod. Phys.* **30** 257 (1958)
160. Hanel G et al. *Phys. Rev. Lett.* **90** 188104 (2003)
161. Denifl S et al. *J. Phys. Chem. A* **108** 6562 (2004)
162. Schiedt J et al. *Chem. Phys.* **239** 511 (1998)
163. Gallup G A, Fabrikant I I *Phys. Rev. A* **83** 012706 (2011)
164. Burrow P D et al. *J. Chem. Phys.* **124** 124310 (2006)
165. Janečková R et al. *Phys. Rev. Lett.* **111** 213201 (2013)
166. Gallup G A, Burrow P D, Fabrikant I I *Phys. Rev. A* **79** 042701 (2009)
167. Kim H, Keller R, Gwinn W D *J. Chem. Phys.* **37** 2748 (1962)
168. Pshenichnyuk S A et al. *Phys. Rev. A* **100** 012708 (2019)
169. Voora V K, Jordan K D *J. Phys. Chem. A* **118** 7201 (2014)
170. Voora V K, Jordan K D *J. Phys. Chem. Lett.* **6** 3994 (2015)
171. Rogers J P, Anstöter C S, Verlet J R R *Nat. Chem.* **10** 341 (2018)
172. Bull J N, Verlet J R R *Sci. Adv.* **3** e1603106 (2017)
173. Sommerfeld T et al. *J. Chem. Phys.* **133** 114301 (2010)
174. Bull J N, Anstöter C S, Verlet J R R *Nat. Commun.* **10** 5820 (2019)
175. Houfek K, Rescigno T N, McCurdy C W *Phys. Rev. A* **77** 012710 (2008)
176. Tarana M et al. *Phys. Rev. A* **84** 052717 (2011)
177. Tennyson J *Phys. Rep.* **491** 29 (2010)
178. Tennyson J et al. *J. Phys. Conf. Ser.* **86** 012001 (2007)
179. Cooper B et al. *Atoms* **7** (4) 97 (2019)
180. Munro J J et al. *J. Phys. Conf. Ser.* **388** 012013 (2012)
181. Kurepa M V, Belic D S *J. Phys. B* **11** 3719 (1978)
182. Carr J M et al. *Eur. Phys. J. D* **66** 58 (2012)
183. Gorfinkiel J D *Eur. Phys. J. D* **74** 51 (2020)
184. Huo W M, Gianturco F A (Eds) *Computational Methods for Electron-Molecule Collisions* (New York: Plenum Press, 1995)
185. Schneider B I, Gharibnejad H *Nat. Rev. Phys.* **2** 89 (2020)
186. Schneider B I, Rescigno T N *Phys. Rev. A* **37** 3749 (1988)
187. Takatsuka K, McKoy V *Phys. Rev. A* **30** 1734 (1984)
188. da Costa R F et al. *Eur. Phys. J. D* **69** 159 (2015)
189. Grimme S *Angew. Chem. Int. Ed.* **52** 6306 (2013)
190. Ásgeirsson V, Bauer C A, Grimme S *Chem. Sci.* **8** 4879 (2017)
191. Bauer C A, Grimme S *J. Phys. Chem. A* **120** 3755 (2016)
192. Pshenichnyuk S A et al. *Phys. Chem. Chem. Phys.* **20** 22272 (2018)
193. Pshenichnyuk S A, Vorob'ev A S, Modelli A *J. Chem. Phys.* **135** 184301 (2011)
194. Ásgeirsson V, Bauer C A, Grimme S *Phys. Chem. Chem. Phys.* **18** 31017 (2016)
195. Flosadóttir H D et al. *Phys. Chem. Chem. Phys.* **13** 15283 (2011)
196. Ómarsson B et al. *Phys. Chem. Chem. Phys.* **15** 4754 (2013)
197. Feng W L, Tian S X *Int. J. Mass Spectrom.* **399** 40 (2016)
198. Zhang Y et al. *Sci. Rep.* **9** 19532 (2019)
199. Modelli A *Phys. Chem. Chem. Phys.* **5** 2923 (2003)
200. Kossoski F, Varella M D N, Barbatti M *J. Chem. Phys.* **151** 224104 (2019)
201. Goursaud S, Sizun M, Fiquet-Fayard F *J. Chem. Phys.* **65** 5453 (1976)
202. Lehr L, Manz J, Miller W H *Chem. Phys.* **214** 301 (1997)
203. Goursaud S, Sizun M, Fiquet-Fayard F *J. Chem. Phys.* **68** 4310 (1978)
204. McAllister M et al. *J. Phys. Chem. B* **123** 1537 (2019)
205. Frisch M J et al., Gaussian 09, Revision A.02 (Wallingford, CT: Gaussian, Inc., 2009)
206. Granovsky A A *J. Chem. Phys.* **134** 214113 (2011)
207. Simons J, Jordan K D *Chem. Rev.* **87** 535 (1987)
208. Staley S W, Strnad J T *J. Phys. Chem.* **98** 116 (1994)
209. Chen D, Gallup G A *J. Chem. Phys.* **93** 8893 (1990)
210. Sanche L, Schulz G J *Phys. Rev. A* **5** 1672 (1972)

211. Sanche L, Schulz G J *Phys. Rev. A* **6** 69 (1972)
212. Scheer A M et al. *J. Phys. Chem. A* **118** 7242 (2013)
213. Burrow P D, Gallup G A, Modelli A *J. Phys. Chem. A* **112** 4106 (2008)
214. Aflatooni K, Gallup G A, Burrow P D *J. Phys. Chem. A* **104** 7359 (2000)
215. Modelli A et al. *J. Phys. Chem. A* **108** 7440 (2004)
216. Pshenichnyuk S A et al. *Phys. Rev. Res.* **2** 012030 (2020)
217. Beynon J H *Mass Spectrometry and its Applications to Organic Chemistry* (Amsterdam: Elsevier, 1960); Translated into Russian: *Mass-spektrometriya i ee Primenenie v Organicheskoi Khimii* (Moscow: Mir, 1964)
218. Asfandiarov N L et al. *J. Chem. Phys.* **147** 234302 (2017)
219. Asfandiarov N L et al. *J. Chem. Phys.* **150** 114304 (2019)
220. Massey H S W *Negative Ions* (Cambridge: Cambridge Univ. Press, 1976); Translated into Russian: *Otritsatel'nie Iony* (Moscow: Mir, 1979)
221. Bardsley J N, Herzenberg A, Mandl F *Proc. Phys. Soc.* **89** 305 (1966)
222. Faddeev L D, Merkuriev S P *Quantum Scattering Theory for Several Particles Systems* (Dordrecht: Kluwer Acad. Publ., 1993); Translated from Russia: Merkuriev S P, Faddeev L D *Kvantovaya Teoriya Rasseyaniya dlya Sistem Neskol'kikh Chastits* (Moscow: Nauka, 1985)
223. Asfandiarov N L "Konkurentsiya dissotsiatsii i avtootshchepleniya elektrona v protsessakh raspada otritsatel'nykh ionov obrazovannykh pri zakhvate elektronov nizkikh energii" ("Competition of dissociation and electron autodetachment during the decay of negative ions produced upon the low-energy electron attachment"), Doctoral Dissertation Phys.-Math. Sciences (Moscow: MSU, 2010)
224. Naff W T, Compton R N, Cooper C D *J. Chem. Phys.* **54** 212 (1971)
225. Compton R N et al. *J. Chem. Phys.* **45** 4634 (1966)
226. Harland P W, Thynne J C J *Inorg. Nucl. Chem. Lett.* **7** 29 (1971)
227. Harland P W, Thynne J C J *J. Phys. Chem.* **75** 3517 (1971)
228. Klots C E *J. Chem. Phys.* **46** 1197 (1967)
229. Odom R W, Smith D L, Futrell J H *J. Phys. B* **8** 1349 (1975)
230. Cannon M et al. *J. Chem. Phys.* **127** 064314 (2007)
231. Liu Y, Suess L, Dunning F B *J. Chem. Phys.* **122** 214313 (2005)
232. Rajput J, Lammich L, Andersen L H *Phys. Rev. Lett.* **100** 153001 (2008)
233. Shchukin P V, Muftakhov M V, Mazunov V A, in *Proc. of the 22nd All-Russia School-Symp. of Young Scientists on Chemical Kinetics, Moscow, 2004*, p. 29
234. Lorquet J C *Mass Spectrom. Rev.* **13** 233 (1994)
235. Robinson P J, Holbrook K A *Unimolecular Reactions* (London: Wiley-Interscience, 1972)
236. Vorob'ev A S et al. *Tech. Phys.* **54** 1255 (2009); *Zh. Tekh. Fiz.* **79** (9) 11 (2009)
237. Christophorou L G *Adv. Electron. Electron Phys.* **46** 55 (1978)
238. Pshenichnyuk S A et al. *J. Chem. Phys.* **132** 244313 (2010)
239. Vorob'ev A S et al. *Tech. Phys.* **59** 1277 (2014); *Zh. Tekh. Fiz.* **84** (9) 17 (2014)
240. Shchukin P V et al. *Int. J. Mass Spectrom.* **273** 1 (2008)
241. Khatymov R V et al. *Int. J. Mass Spectrom.* **303** 55 (2011)
242. Khatymov R V et al. *Phys. Chem. Chem. Phys.* **22** 3073 (2020)
243. Asfandiarov N L et al. *Rapid Commun. Mass Spectrom.* **28** 1580 (2014)
244. Stockdale J A D, Compton R N, Schweinler H C *J. Chem. Phys.* **53** 1502 (1970)
245. Christophorou L G *Atomic and Molecular Radiation Physics* (London: Wiley-Interscience, 1971)
246. Thynne J C J, Harland P W *Int. J. Mass Spectrom. Ion Phys.* **11** 137 (1973)
247. Henis J M S, Mabie C A *J. Chem. Phys.* **53** 2999 (1970)
248. Naff W T, Cooper C D, Compton R N *J. Chem. Phys.* **49** 2784 (1968)
249. Johnson J P et al. *J. Chem. Soc. Faraday Trans. 2* **71** 1742 (1975)
250. Pshenichnyuk S A et al. *Mass-spektrometriya* **2** 317 (2005)
251. Pshenichnyuk S A, Asfandiarov N L, Kukhto A V *Khim. Fiz.* **26** 5 (2007)
252. Presnyak V A *Vestn. St.-Peterburg. Univ. Ser. 1* (2) 116 (2010)
253. Herzberg G *Infrared and Raman Spectra of Polyatomic Molecules* (New York: Van Nostrand, 1945); Translated into Russian: *Kolebatel'nye i Vrashchatel'nye Spektry Mnogoatomnykh Molekul* (Moscow: IL, 1949)
254. Pshenichnyuk S A "Rezonansnyi zakhvat elektronov molekulami organicheskikh soedinenii: eksperiment, fundamental'nye aspekty i vozmozhnye prilozheniya v molekulyarnoi elektronike i biokhimii" ("Resonance electron attachment by organic molecules: experiment fundamental aspects and possible applications in molecular electronics and biochemistry", Doctoral Dissertation Phys.-Math. Sciences (Ufa: Bashkir State Univ., 2017)
255. Kočišek J et al. *J. Phys. Chem. Lett.* **7** 3401 (2016)
256. Kočišek J et al. *Eur. Phys. J. D* **70** 1 (2016)
257. Pimblott S M, LaVerne J A *Radiat. Phys. Chem.* **76** 1244 (2007)
258. Alizadeh E, Orlando T M, Sanche L *Annu. Rev. Phys. Chem.* **66** 379 (2015)
259. Sanche L *Mass Spectrom. Rev.* **21** 349 (2002)
260. Martin F et al. *Phys. Rev. Lett.* **93** 068101 (2004)
261. Friedberg E C *Nature* **421** 436 (2003)
262. Zheng Y, Sanche L *Rev. Nanosci. Nanotechnol.* **2** 1 (2013)
263. Kopyra J et al. *Angew. Chem. Int. Ed.* **48** 7904 (2009)
264. Bao Q et al. *J. Phys. Chem. C* **118** 15516 (2014)
265. Rackwitz J et al. *Angew. Chem.* **128** 10404 (2016)
266. Cheng H Y et al. *Comp. Theor. Chem.* **1075** 18 (2016)
267. Huber S E et al. *J. Chem. Phys.* **144** 224309 (2016)
268. Makurat S, Chomicz-Mańka L, Rak J *Chem. Phys. Chem.* **17** 2572 (2016)
269. Lange E et al. *J. Phys. Conf. Ser.* **635** 072069 (2015)
270. Schürmann R et al. *J. Phys. Chem. B* **121** 5730 (2017)
271. Tanzer K et al. *Int. J. Mass Spectrom.* **365** 152 (2014)
272. Ribar A et al. *Chem. Eur. J.* **23** 12892 (2017)
273. Ončák M et al. *Int. J. Mol. Sci.* **20** 4383 (2019)
274. Aflatooni K et al. *J. Chem. Phys.* **115** 6489 (2001)
275. Scheer A M et al. *J. Chem. Phys.* **126** 174301 (2007)
276. Papp P, Shchukin P, Matejčík Š *J. Chem. Phys.* **132** 014301 (2010)
277. Muftakhov M V, Shchukin P V *Phys. Chem. Chem. Phys.* **13** 4600 (2011)
278. Muftakhov M V, Shchukin P V *Rapid Commun. Mass Spectrom.* **30** 2577 (2016)
279. Muftakhov M V, Shchukin P V *Izv. Akad. Nauk, Ser. Khim.* **9** 1675 (2019)
280. Muftakhov M V, Shchukin P V *Rapid Commun. Mass Spectrom.* **33** 482 (2019)
281. Muftakhov M V, Shchukin P V, Khatymov R V *Zh. Fiz. Khim.* **91** 1534 (2017)
282. Solov'yov A V (Ed.) *Nanoscale Insights into Ion-Beam Cancer Therapy* (Cham: Springer Intern. Publ., 2017)
283. Baccarelli I et al. *Phys. Rep.* **508** 1 (2011)
284. Gorfinkiel J D, Ptasinska S *J. Phys. B* **50** 182001 (2017)
285. Kumar A et al. *Int. J. Mol. Sci.* **20** 3998 (2019)
286. Postulka J et al. *J. Phys. Chem. B* **121** 8965 (2017)
287. McAllister M et al. *J. Phys. Chem. Lett.* **6** 3091 (2015)
288. Westphal K et al. *Org. Biomol. Chem.* **13** 10362 (2015)
289. Shao Y et al. *J. Phys. Chem. C* **121** 2466 (2017)
290. Mathur D *J. Phys. B* **48** 022001 (2014)
291. McFadden J, Al-Khalili J *Proc. R. Soc. A* **474** 20180674 (2018)
292. Cao J et al. *Sci. Adv.* **6** eaaz4888 (2020)
293. Pshenichnyuk S A, Modelli A, Komolov A S *Int. Rev. Phys. Chem.* **37** 125 (2018)
294. Szent-Györgyi A *Science* **93** 609 (1941)
295. Lovelock J E *Nature* **189** 729 (1961)
296. Getoff N *Hormone Molec. Biol. Clinical Invest.* **16** 125 (2013)
297. Getoff N *In Vivo* **28** 61 (2014)
298. Chen Q et al. *J. Biol. Chem.* **278** 36027 (2003)
299. Murphy M P *Biochem. J.* **417** 1 (2009)
300. Hannemann F et al. *Biochim. Biophys. Acta BBA General Sub.* **1770** 330 (2007)
301. Denisov I G et al. *Chem. Rev.* **105** 2253 (2005)
302. Ervin K M et al. *J. Phys. Chem. A* **107** 8521 (2003)
303. Rotko G et al. *Electrochem. Commun.* **43** 117 (2014)
304. Saveant J M *Acc. Chem. Res.* **26** 455 (1993)
305. Antonello S, Maran F *Chem. Soc. Rev.* **34** 418 (2005)
306. Brett A M O, Ghica M E *Electroanalysis* **15** 1745 (2003)
307. Recknagel R O et al. *Pharmacol. Therapeut.* **43** 139 (1989)
308. Schweizer S, Rusling J F, Huang Q *Chemosphere* **28** 961 (1994)

309. Rotko G, Romańczyk P P, Kurek S S *Electrochem. Commun.* **37** 64 (2013)
310. Firuzi O et al. *Biochim. Biophys. Acta BBA General Sub.* **1721** 174 (2005)
311. Pshenichnyuk S A, Modelli A *Phys. Chem. Chem. Phys.* **15** 9125 (2013)
312. Bussy U, Boujtita M *Chem. Res. Toxicol.* **27** 1652 (2014)
313. Shumyantseva V V et al. *Biosens. Bioelectron.* **121** 192 (2018)
314. Syroeshkin M A et al. *Angew. Chem. Int. Ed.* **58** 5532 (2019)
315. Staneke P O et al. *Int. J. Mass Spectrom. Ion Proc.* **142** 83 (1995)
316. Recknagel R O *Pharmacol. Rev.* **19** 145 (1967)
317. Brattin W J, Glende E A (Jr.), Recknagel R O *J. Free Radicals Biol. Med.* **1** 27 (1985)
318. Chu S C, Burrow P D *Chem. Phys. Lett.* **172** 17 (1990)
319. Gregory N L *Nature* **212** 1460 (1966)
320. Gutteridge J M, Halliwell B *Trends Biochem. Sci.* **15** 129 (1990)
321. Basu S *Toxicol.* **189** 113 (2003)
322. Modelli A, Pshenichnyuk S A *J. Phys. Chem. A* **116** 3585 (2012)
323. Pshenichnyuk S A, Lomakin G S, Modelli A *Phys. Chem. Chem. Phys.* **13** 9293 (2011)
324. Pshenichnyuk S A et al. *J. Phys. Chem. B* **120** 12098 (2016)
325. Demidchik V *Environ. Experim. Botan.* **109** 212 (2015)
326. Pshenichnyuk S A, Komolov A S *J. Phys. Chem. B* **121** 749 (2017)
327. Modelli A, Pshenichnyuk S A *Phys. Chem. Chem. Phys.* **15** 1588 (2013)
328. Pshenichnyuk S A et al. *Phys. Chem. Chem. Phys.* **17** 16805 (2015)
329. Pshenichnyuk S A, Komolov A S *J. Phys. Chem. Lett.* **6** 1104 (2015)
330. Asfandiarov N L et al. *Int. J. Mass Spectrom.* **412** 26 (2017)
331. Pshenichnyuk S A, Komolov A S *J. Phys. Chem. Lett.* **5** 2916 (2014)
332. Pshenichnyuk S A et al. *J. Phys. Chem. B* **121** 3965 (2017)
333. Pshenichnyuk S A et al. *J. Phys. Chem. A* **120** 2667 (2016)
334. Muftakhov M V, Shchukin P V *Chem. Phys. Lett.* **739** 136967 (2020)
335. Hendrickson H P, Kaufman A D, Lunte C E *J. Pharmaceut. Biomed. Analys.* **12** 325 (1994)
336. Heim K E, Tagliaferro A R, Bobilya D J *J. Nutrition. Biochem.* **13** 572 (2002)
337. Leopoldini M, Russo N, Toscano M *Food Chem.* **125** 288 (2011)
338. Pshenichnuyk S A et al. *Pis'ma Mater.* **5** 504 (2015)
339. Ohsawa I et al. *Nat. Med.* **13** 688 (2007)
340. Hong Y, Chen S, Zhang J M *J. Int. Med. Res.* **38** 1893 (2010)
341. Cochemé H M et al. *Mitochondrion* **7** S94 (2007)
342. Weissig V *Trends Mol. Med.* **26** 40 (2020)
343. Pshenichnyuk S A, Modelli A, in *Mitochondrial Medicine* Vol. 3 (Methods in Molecular Biology, Vol. 2277, Eds V Weissig, M Edeas) 2nd ed. (New York: Springer, Humana Press, 2021) p. 101
344. Pshenichnyuk S A, Modelli A *J. Chem. Phys.* **136** 234307 (2012)
345. Lee E K et al. *Adv. Mater.* **29** 1703638 (2017)
346. Zhou W et al. *Nano Lett.* **14** 1614 (2014)
347. Modelli A, Burrow P D *J. Phys. Chem. A* **115** 1100 (2011)
348. Tuktarov R F et al. *JETP Lett.* **96** 664 (2012); *Pis'ma Zh. Eksp. Teor. Fiz.* **96** 738 (2012)
349. Pshenichnyuk S A et al. *J. Phys. Chem. A* **118** 6810 (2014)
350. Pshenichnyuk S A et al. *Tech. Phys.* **56** 754 (2011); *Zh. Tekh. Fiz.* **81** (6) 8 (2011)
351. Pshenichnyuk S A, Komolov A S *J. Phys. Chem. A* **116** 761 (2012)
352. Pshenichnyuk S A et al. *Russ. J. Phys. Chem. B* **4** 1014 (2010); *Khim. Fiz.* **29** (11) 82 (2010)
353. Khatymov R V, Muftakhov M V, Shchukin P V *Rapid Commun. Mass Spectrom.* **31** 1729 (2017)
354. Muftakhov M V, Khatymov R V, Tuktarov R F *Tech. Phys.* **63** 1854 (2018); *Zh. Tekh. Fiz.* **88** 1893 (2018)
355. Pshenichnyuk I A, Kosolobov S S, Drachev V P *Appl. Sci.* **9** 4834 (2019)
356. Kao C Y et al. *Organic Lett.* **16** 6100 (2014)
357. Kudernac T et al. *Nature* **479** 208 (2011)
358. Kottas G S et al. *Chem. Rev.* **105** 1281 (2005)
359. Pshenichnyuk S A, Asfandiarov N L, Kukhta A V *Phys. Rev. A* **86** 052710 (2012)
360. Pshenichnyuk S A, Asfandiarov N L *Phys. Chem. Chem. Phys.* **22** 16150 (2020)
361. Pshenichnyuk I A, Ćížek M *Phys. Rev. B* **83** 165446 (2011)
362. Pshenichnyuk I A et al. *J. Phys. Chem. Lett.* **4** 809 (2013)
363. Komolov S A, Chadderton L T *Surf. Sci.* **90** 359 (1979)
364. Kaur N et al. *Synth. Met.* **190** 20 (2014)
365. Dou L et al. *Chem. Rev.* **115** 12633 (2015)
366. Lachinov A N, Vorob'eva N V *Phys. Usp.* **49** 1223 (2006); *Usp. Fiz. Nauk* **176** 1249 (2006)
367. Shirakawa H, Ikeda S *Synth. Met.* **1** 175 (1980)
368. Salazkin S N *Polym. Sci. B* **46** (7–8) 203 (2004); *Vysokomol. Soed. B* **46** 1244 (2004)
369. Vasil'sev Y V et al. *Synth. Met.* **84** 975 (1997)
370. Asfandiarov N L et al. *J. Chem. Phys.* **142** 174308 (2015)
371. Pshenichnyuk S A et al. *J. Chem. Phys.* **151** 214309 (2019)
372. Asfandiarov N L et al. *J. Chem. Phys.* **151** 134302 (2019)
373. Christophorou L G, Gant K S, Anderson V E *J. Chem. Soc. Faraday Trans.* **2** 804 (1977)
374. Matejčik Š et al. *J. Chem. Phys.* **102** 2516 (1995)
375. Asfandiarov N L et al. *Rapid Commun. Mass Spectrom.* **29** 910 (2015)
376. Hahndorf I et al. *Chem. Phys. Lett.* **231** 460 (1994)
377. Pearl D M et al. *J. Chem. Phys.* **102** 2737 (1995)
378. Neporent B S, Stepanov B I *Usp. Fiz. Nauk* **43** 380 (1951)
379. Klots C E *J. Chem. Phys.* **90** 4470 (1989)
380. Klots C E *J. Chem. Phys.* **93** 2513 (1990)
381. Lifshitz C, Tiernan T O, Hughes B M *J. Chem. Phys.* **59** 3182 (1973)
382. Lifshitz C et al. *J. Chem. Phys.* **53** 4605 (1970)
383. Koval'skaya G A, Petrov A K, Kuibida L V *Khim. Fiz.* **24** (6) 14 (2005)
384. Bray R G, Berry M J *J. Chem. Phys.* **71** 4909 (1979)
385. Malinovskii A L, Makarov A A, Ryabov E A *JETP Lett.* **80** 532 (2004); *Pis'ma Zh. Eksp. Teor. Fiz.* **80** 605 (2004)
386. Asfandiarov N L et al. *Russ. J. Phys. Chem.* **91** 915 (2017); *Zh. Fiz. Khim.* **91** 880 (2017)
387. Asfandiarov N et al., in *Book of Contributed Papers of the 20th Symp. on Application of Plasma Processes, Tatranská Lomnica, Slovakia, 2015*, p. 39
388. Kalimullina L R et al. *Russ. J. Phys. Chem.* **89** 429 (2015); *Zh. Fiz. Khim.* **89** 426 (2015)
389. Zhu X Q, Wang, C H *J. Org. Chem.* **75** 5037 (2010)
390. Corderman R R, Lineberger W C *Annu. Rev. Phys. Chem.* **30** 347 (1979)
391. Engelking P C, Lineberger W C *J. Chem. Phys.* **67** 1412 (1977)
392. Chen E S, Chen E C *Rapid Commun. Mass Spectrom.* **32** 604 (2018)
393. Goryunkov A A et al. *J. Phys. Chem. A* **124** 690 (2020)
394. Ponomarev O A, Mazunov V A *Bull. Acad. Sci. USSR Div. Chem. Sci.* **35** 320 (1986); *Izv. Akad. Nauk SSSR Ser. Khim.* (2) 347 (1986)
395. Khatymov R V et al. *J. Chem. Phys.* **150** 134301 (2019)
396. Laikov D N *Chem. Phys. Lett.* **416** 116 (2005)
397. Collins P M et al. *Chem. Phys. Lett.* **4** 646 (1970)
398. Vasil'ev Yu V, Mazunov V A *JETP Lett.* **51** 144 (1990); *Pis'ma Zh. Eksp. Teor. Fiz.* **51** 129 (1990)
399. Cooper C D, Naff W T, Compton R N *J. Chem. Phys.* **63** 2752 (1975)
400. Pshenichnyuk S A et al. *Rapid Commun. Mass Spectrom.* **20** 383 (2006)
401. Compton R N, Cooper C D *J. Chem. Phys.* **66** 4325 (1977)
402. Khvostenko O G, Tuimedov G M *Rapid Commun. Mass Spectrom.* **20** 3699 (2006)
403. Ponomarev O A, Mazunov V A *Khim. Fiz.* **5** 226 (1986)
404. Sommerfeld T, Davis M C *J. Chem. Phys.* **149** 084305 (2018)
405. Tuktarov R F et al. *JETP Lett.* **81** 171 (2005); *Pis'ma Zh. Eksp. Teor. Fiz.* **81** 207 (2005)
406. Vasil'ev Y V, Tuktarov R F, Mazunov V A *Rapid Commun. Mass Spectrom.* **11** 757 (1997)
407. Tuktarov R F et al. *JETP Lett.* **90** 515 (2009); *Pis'ma Zh. Eksp. Teor. Fiz.* **90** 564 (2009)
408. Vasil'ev Y V et al. *Int. J. Mass Spectrom. Ion Process.* **173** 113 (1998)
409. Ipatov A N "Kollektivnye elektronnye vozbuzdeniya v atomnykh klasterakh i molekulakh" ("Collective electronic excitations in atomic clusters and molecules"), Doctoral Dissertation Phys.-Math. Sciences (St. Petersburg: St. Petersburg State Univ., 2010)
410. Vasil'ev Y V et al. *Fullerenes Nanotubes Carbon Nanostruct.* **12** 229 (2005)
411. Freed K F, Jortner J *J. Chem. Phys.* **50** 2916 (1969)
412. Ermolaev V L *Russ. Chem. Rev.* **70** 471 (2001); *Usp. Khim.* **70** 539 (2001)

413. Jortner J, Berry R S *J. Chem. Phys.* **48** 2757 (1968)
414. Khvostenko V I et al. *Dokl. Akad. Nauk SSSR* **213** 1364 (1973)
415. Medvedev E S, Osherov V I *Radiationless Transitions in Polyatomic Molecules* (Berlin: Springer-Verlag, 1995); Translated from Russian: *Teoriya Bezizluchatel'nykh Perekhodov v Mnogoatgomnykh Molekulakh* (Moscow: Nauka, 1983)
416. Neustetter M et al. *Angew. Chem. Int. Ed.* **54** 9124 (2015)
417. Ahlenhoff K et al. *Phys. Chem. Chem. Phys.* **21** 2351 (2019)
418. Scheuerer P, Patera L L, Repp J *Nano Lett.* **20** 1839 (2020)
419. Nesbitt D J, Field R W *J. Phys. Chem.* **100** 12735 (1996)
420. Makarov A A, Malinovsky A L, Ryabov E A *Phys. Usp.* **55** 977 (2012); *Usp. Fiz. Nauk* **182** 1047 (2012)
421. Stannard P R, Gelbart W M *J. Phys. Chem.* **85** 3592 (1981)
422. Boyall D, Reid K L *Chem. Soc. Rev.* **26** 223 (1997)
423. Panek P T, Jacob C R *Chem. Phys. Chem.* **15** 3365 (2014)
424. Gauyacq J P, Herzenberg A *J. Phys. B* **17** 1155 (1984)
425. Ovchinnikov A A, Erikhman N S *Sov. Phys. Usp.* **25** 738 (1982); *Usp. Fiz. Nauk* **138** 289 (1982)
426. Kraka E, Zou W, Tao Y *WIREs Comput. Mol. Sci.* **10** e1480 (2020)
427. Kunitsa A A, Bravaya K B *J. Phys. Chem. Lett.* **6** 1053 (2015)
428. Gertitschke P L, Domcke W *Phys. Rev. A* **47** 1031 (1993)
429. Slaughter D S et al. *J. Phys. B* **49** 222001 (2016)
430. Chakraborty D, Nag P, Nandi D *Rev. Sci. Instrum.* **89** 025115 (2018)
431. Kohanoff J et al. *J. Phys. Condens. Matter* **29** 383001 (2017)
432. Auría-Soro C et al. *Nanomaterials* **9** 1365 (2019)
433. Yin H et al. *Small* **15** 1903674 (2019)
434. Zhang Y et al. *Chem. Rev.* **118** 2927 (2018)
435. Schürmann R, Bald I *Nanoscale* **9** 1951 (2017)
436. Schürmann R et al. *J. Chem. Phys.* **153** 104303 (2020)